THE UNIVERSITY OF CHICAGO

THE GENETIC BASIS AND EVOLUTION OF POLYMORPHIC MIMICRY IN SWALLOWTAIL BUTTERFLIES

A DISSERTATION SUBMITTED TO

THE FACULTY OF THE DIVISION OF THE BIOLOGICAL SCIENCES

AND THE PRITZKER SCHOOL OF MEDICINE

IN CANDIDACY FOR THE DEGREE OF

DOCTOR OF PHILOSOPHY

COMMITTEE ON EVOLUTIONARY BIOLOGY

BY

DANIELA HELENA DROGUETT PALMER

CHICAGO, ILLINOIS

JUNE 2018

Contents

List of Figures

List of Tables

Acknowledgments

This work would not have been possible without the guidance, support, and encouragement of many people. First, my thesis advisor, Dr. Marcus Kronforst, was central to my development as a scientist. Working with Dr. Kronforst and other members of the Kronforst lab community afforded me crucial opportunities to engage in different types of science, and these experiences have truly defined my ways of thinking about biological systems. My thesis committee was another integral part of this development, and I am grateful for their thoughtful input and enthusiasm – Dr. Trevor Price, Dr. Corrie Moreau, and Dr. Urs Schmidt-Ott. As a dual member of the Committee on Evolutionary Biology and the Department of Ecology and Evolution at the University of Chicago, I have been fortunate to interact with a broad network of people that fostered my success as a graduate student. Dr. Michael Coates, Dr. Shannon Hackett, Dr. Carolyn Johnson, and Dr. Elizabeth Eakin provided critical support numerous times, as did staff members Bonnie Brown, Jeff Wisniewski, Mary Johnson, Garnett Kirk, and Mike Guerra. The greenhouse staff, Sandra Suwanski and John Zdenek, was essential to maintaining the animals that made this work possible. Many members of the University of Chicago Functional Genomics Facility also were helpful with technical advice.

The field work I conducted was a substantial part of my scientific development. I thank Dr. Antónia Monteiro and members of her lab for hosting me in Singapore and helping me navigate the new environment. I also thank Singapore NParks and National Research Foundation for their assistance in logistical planning.

During my time at the University of Chicago I was financially supported by various sources. I was able to conduct field research in Singapore thanks to the National Science

Foundation East Asia and Pacific Summer Insitutes (#IIA-1414798). In years two through six of graduate school I was a Fellow of the Department of Education Graduate Assistance in Areas of National Need Training Grant. I thank the faculty and administrators that made this funding available to me.

Finally, there are a multitude of individuals to thank that had impacts on me personally and professionally during my graduate school experience and helped me complete this milestone in my life: Dr. Erica Westerman, Dr. Darli Massardo, Dr. Wei Zhang, Dr. Nicholas VanKuren, Dr. Delbert André Green II, Dr. Sumitha Nallu, Dr. Daniel Hooper, Dr. Joyce Pieretti, Dr. Thomas Stewart, Dr. Alexandria Bobé, Dr. Simon Lax, Dr. Susan Finkbeiner, Erick Bayala, Roberto Marquez, Ayse Tenger-Trolander, Laura Southcott, Carlos Sahagun, Victoria Flores, Dallas Krentzel, Carlos Cardenas-Iñiguez, Natalia Piland, Joel Mercado Diaz, Pamela Martinez, Mauricio Santos, Supriya, Gabriel Vargas, and Alex White. I have to express my gratitude to members of my family that motivated me to pursue this path: Abuelito Oscar, Jacqueline Droguett, Bennett Palmer, Benjamin Palmer, Tia Lili, Tio Enrique, Tio Oscar, Karime, Tio Arturo, primo Enrique, primo Oscar, Erika, prima Fra, Ani. Finally, Shane DuBay was a true partner and advocate throughout my time as a graduate student, and I am deeply appreciative of everything he has patiently done for me and helped me achieve.

Introduction

A major goal in evolutionary genetics is to understand the molecular changes underlying adaptations and the evolutionary processes that have shaped adaptation and biodiversity. To this end, the ability to pinpoint the genetic basis of complex adaptive phenotypes has been a major advancement in current biology. Classic biological systems are being revisited with a genomics lens, building on traditional approaches in evolution, ecology, and natural history (Shapiro et al., 2004; Gompel et al., 2005; Prud'homme et al., 2006; Nadeau and Jiggins, 2011; Reed et al., 2011; Brawand et al., 2014; Kunte, Zhang et al., 2014; Lamichhaney et al., 2015; Li et al., 2016). By applying new genomic methods to classic biological questions, we are making progress along two major fronts: uncovering the genes, molecular mechanisms, and genetic architectures that generate adaptive phenotypes, and exploring the evolutionary processes that give rise to these adaptations.

New genomic methods have facilitated the discovery of genes underlying complex adaptations. These discoveries, in turn, have tackled longstanding questions about natural selection and the process of adaptation, including whether adaptation is driven by small, gradual changes among many genes or by few genes with large effects, and whether these changes tend to be cis- or trans-acting. A large source of adaptive variation, for example, is found in animal coloration, and several systems of animal coloration have now been characterized at the genetic level. Much of the variation in adaptive coloration across invertebrate and vertebrate systems has been found to stem from changes at relatively few genes, and a variety of regulatory and structural molecular mechanisms have been attributed to adaptive coloration (Papa et al., 2008; Kronforst et al., 2012; San-Jose and Roulin, 2017). The research on animal coloration illustrates

how advances in methodology have promoted our understanding of evolutionary processes by leveraging genomic datasets to empirically test theoretical hypotheses.

The advent of genomic methods has spurred not only the discovery of genes underlying complex adaptations, but also the characterization of how those genes are organized in the genome (Ellegren, 2014). A significant, recurring theme in the organization and maintenance of adaptive variation is the widespread role of chromosomal inversions in maintaining polymorphisms within species and locally adapted phenotypes (Hoffman and Rieseberg, 2008; Faria and Navarro, 2010; Lowry and Willis, 2010). Inversions maintain linkage between co-adapted variants because they suppress recombination between homologous regions by physically reversing tracts of DNA along a chromosome (Sturtevant, 1921; Kirkpatrick, 2010). Whether inverted regions encompass one or many genes, the Mendelian inheritance of inverted regions enables the co-segregation of adaptive variation within species. Numerous recent studies have identified this type of genetic architecture underlying complex adaptive traits, including sperm morphology and mating behavior in birds (Küpper et al., 2016; Lamichhaney et al., 2016; Kim et al., 2017; Tuttle et al., 2016), flower reproductive morphology (Li et al., 2016), fire ant social behavior (Wang et al., 2013), and wing pattern polymorphism in several butterfly groups (Kunte, Zhang et al., 2014; Nishikawa et al., 2015; Timmermans et al., 2014; Timmermans et al., 2017; Joron et al., 2006; Joron et al., 2011). While it is still unclear whether inversions occur as a cause or consequence of reduced recombination between haplotypes (Schwander et al., 2014), their common presence seems to indicate an important evolutionary role in maintaining the traits that they encompass. Furthermore, this genetic architecture appears to facilitate the spread of haplotypes across species boundaries, linking inversions to adaptive introgression as a driving force in phenotypic evolution (Schwander et al., 2014).

Uncovering the genomic basis of adaptive phenotypes also allows us to disentangle the roles of historical and genetic factors in shaping adaptation by comparing relevant loci to the rest of the genome. Systems that exhibit convergence, where multiple organisms have evolved similar traits, offer a particularly promising framework in which to test when and how natural selection, phylogenetic history, demography, and constraint have shaped patterns of adaptive biodiversity (Rosenblum et al., 2014). By contrasting the phylogenetic signatures inferred from different parts of the genome – those directly involved in adaptation versus those not – we have come to recognize the widespread contributions of introgression and incomplete lineage sorting to adaptation (Ellegren, 2014; Palmer and Kronforst, 2015). Fukushima et al. (2017) recently implemented such a framework to study the origins of plant carnivory, showing how genetic constraint has likely driven the parallel molecular pathways involved in the repeated evolution of this adaptation. Conversely, Harrison et al. (2018) showed how differences in the ancestral repertoires of chemoreceptors between termites and Hymenoptera favored similar but distinct molecular paths toward eusociality. These studies are part of a growing body of research that is propelling our understanding of the pivotal effects of genetic and historical factors on evolution.

There is no doubt that high-throughput sequencing technologies have marked a new era in the life sciences. However, it is critical to establish links between genotypes, phenotypes, and evolutionary processes if we are to study adaptive biodiversity. It is perhaps no wonder that some of the most fruitful evolutionary genomics works have focused on biological systems with rich traditions of evolution, ecology, and natural history. These systems provide a robust foundation that anchors signatures of genomic variation to organismal adaptation. For example, the work on Darwin's finches, which I reviewed in Chapter 1, takes the meticulously documented data on seed shape variation, beak shape variation, and finch survivorship over time, and layers on

genomic analyses to learn about adaptive morphological evolution (Lamichhaney et al., 2015). This feedback between disciplines drives a holistic characterization of the evolutionary process, addressing longstanding questions and pushing the boundaries of inquiry by motivating new questions.

Through the work included in this dissertation, I have sought to explore the evolutionary processes that generate and maintain adaptive biodiversity. First, I reviewed new genomics insights on a classic system, Darwin's finches, and connected these findings to the growing literature on adaptive introgression and its contributions to phenotypic evolution (Chapter 1). I then looked to another classic system in evolutionary biology with a long tradition of theoretical and empirical research: polymorphic wing pattern mimicry in *Papilio* swallowtail butterflies. In *Papilio*, I studied i) natural selection on polymorphic wing pattern phenotypes in the field (Chapter 2), and ii) the genetic basis and evolution of convergent polymorphic wing pattern mimicry (Chapter 3).

1 Divergence and gene flow among Darwin's finches: A genome-wide view of adaptive radiation driven by interspecies allele sharing[1]

1.1 Abstract

A recent analysis of the genomes of Darwin's finches revealed extensive interspecies allele sharing throughout the history of the radiation and identified a key locus responsible for morphological evolution in this group. The radiation of Darwin's finches on the Galápagos archipelago has long been regarded as an iconic study system for field ecology and evolutionary biology. Coupled with an extensive history of field work, these latest findings affirm the increasing acceptance of introgressive hybridization, or gene flow between species, as a significant contributor to adaptive evolution. Here we review and discuss these findings in relation to both classical work on Darwin's finches and contemporary work showing similar evolutionary signatures in other biological systems. The continued unification of genomic data with field biology promises to further elucidate the molecular basis of adaptation in Darwin's finches and well beyond.

1.2 Introduction

The fields of ecology, evolutionary biology, and animal behavior are deeply rooted in organismal natural history. For centuries, curious naturalists have observed and catalogued the spectacular biology of diverse plants and animals in their natural environment, and no natural historian is more famous than Charles Darwin, the founder of modern evolutionary theory. In developing his

[1] A version of this chapter has been published as: Palmer DH and MR Kronforst. 2015. Divergence and gene flow among Darwin's finches: A genome-wide view of adaptive radiation driven by interspecies allele sharing. BioEssays 37: 968-974.

theory of evolution by natural selection, Darwin wove together many detailed observations of organismal biology to produce a compelling argument that left little room for doubt regarding his basic tenets of descent with modification and the power of natural selection to produce remarkable phenotypic adaptation (Darwin and Wallace, 1858; Darwin, 1859). Today, as we continue to work out the ancestral relationships among taxa and explore the specific evolutionary processes responsible for adaptation, it is becoming increasingly clear that essential historical clues lie hidden in the genes that control organismal phenotypes (Hoekstra and Coyne, 2007; Stern and Orgogozo, 2008; Stern and Orgogozo, 2009; Martin and Orgogozo, 2013). However, the quest to find these genes is often an arduous one (Barrett and Hoekstra, 2011; Rockman, 2012; Lee et al., 2014; Rausher and Delph, 2015). Genomics research, and the sub-fields of comparative and population genomics specifically, offers huge promise to unlock the molecular basis of biodiversity (Nadeau and Jiggins, 2010; Stapley et al., 2010). With the rapid advance of genome sequencing technology, we appear to be entering a 'golden age' for evolutionary genetics (Nadeau and Jiggins, 2010), one in which the hunt for genes underlying adaptation is progressing rapidly.

Recently, there have been a number of instances in which genomic approaches have produced major insights into classic evolutionary systems and questions, such as the diversification of cichlid (Brawand et al., 2014) and stickleback (Jones et al., 2012) fishes, the evolution of mimicry in *Heliconius* butterflies (Heliconius Genome Consortium, 2012), and the genetics of migration in the monarch butterfly (Zhan et al., 2014). A recent example of the power of population-level genomics to generate new understanding of an age-old question is a recent publication by Lamichhaney et al. (2015) on Darwin's finches. Here, whole-genome sequencing of an entire adaptive radiation has been coupled with a study system that has an extensive record

of field research focused on natural history and ecology. The results reveal the history of diversification and gene flow among species as well as identifying specific genes associated with an iconic morphological adaptation, beak shape. The findings also further unify observational evidence for interspecific hybridization with genetic evidence for adaptive interspecies allele sharing. This study, along with several other recent investigations (Heliconius Genome Consortium, 2012; Fontaine et al., 2015; Huerta-Sanchez et al., 2014; Liu et al., 2015), reinforces the increasing acknowledgement of adaptive introgression as a potentially important and widespread evolutionary phenomenon.

1.3 A tradition of field biology research on Darwin's finches

Darwin's finches are a group of about 14 species that evolved from a common ancestor on the Galápagos archipelago, a 15th species inhabiting Cocos Island (Figure 1). Since Charles Darwin's voyage on the *HMS Beagle*, this radiation has been the focal point of novel insights into evolutionary biology. Darwin's observations of the finch radiation led him to develop foundational ideas about evolution, including descent from a common ancestor, island colonization by mainland species, and adaptive radiation (Darwin, 1859). It was years after the *Beagle* voyage, however, that Darwin received input on the group's morphological variation and systematics from taxonomist John Gould and formulated the insights for which he is famous (Sulloway, 1982). Darwin became particularly drawn to beak shape, and noting the incredible diversity in this trait among the closely related finches, he stated in the second edition of *Journal of Researches (Voyage of the Beagle)* (Darwin, 1845) "Seeing this gradation and diversity of structure in one small, intimately related group of birds, one might really fancy that from an original paucity of birds in this archipelago, one species had been taken and modified for

different ends." Darwin's statement here about the Galápagos finches, 14 years before *On the Origin of Species* (Darwin, 1859), reveals the emergence of his evolutionary thinking much earlier than many realize.

More recently, the detailed work of Peter and Rosemary Grant has established the connection between climatic fluctuation, seed availability, and natural selection on beak morphology (Gibbs and Grant, 1987; Grant and Grant, 1993; Grant and Grant, 2002). Furthermore, their work also documented detailed observations of immigration and hybridization producing viable offspring (Grant and Grant, 2002; Grant, 1993; Grant and Grant, 2010). Additional analyses of song revealed the directionality of gene flow from hybrids into the parental populations (Grant and Grant, 1997a; Grant and Grant, 1997b; Grant and Grant, 1998). The synthesis of 40 years of observations combined with analyses of beak morphology and body size, song, and microsatellite genetic data showed convergent evolution in Darwin's finches owing to introgressive hybridization and natural selection (Grant et al., 2004; Grant and Grant, 2014). Advances by Podos, Huber, Hendry, DeLeón, and colleagues addressed the processes underlying adaptive radiation in Darwin's finches (Podos, 2001; Huber et al., 2007; Hendry et al., 2006; De León et al., 2011). Podos (2001) demonstrated that divergence in beak morphology drove evolution in vocal mating signals, likely promoting reproductive isolation and rapid speciation in the finch radiation. Huber et al. (2007) showed beak size polymorphism in a Santa Cruz Island *G. fortis* population, presumably owing to ecological divergence, and subsequent assortative mating of the two morphs reminiscent of incipient speciation. Parallel studies related these findings to human impacts, showing how increased human population density can reduce the correlations between beak shape, size, bite force, and diet, thereby increasing the frequency

Figure 1 | Representatives of the Darwin's finch radiation. Illustrations from *Birds Part 3 No. 4* (1839) and *Birds Part 3 No. 5* (1841) of *The zoology of the voyage of H.M.S. Beagle* by John Gould, edited by Charles Darwin. Reproduced with permission from John van Wyhe ed. 2002-. The Complete Work of Charles Darwin Online. (http://darwin-online.org.uk/)

of intermediate phenotypes and negatively impacting adaptive radiation (Hendry et al., 2006; De León et al., 2011).

1.4 Genetic insight on beak development reveals the developmental modules underlying morphological change

Previous work by Abzhanov and colleagues (Abzhanov et al., 2006; Abzhanov et al., 2004; Mallarino et al., 2011) has investigated the developmental genetics of beak variation among Darwin's finches. Two anatomical components, the prenasal cartilage (pnc) and premaxillary bone (pmx), determine adult beak morphology. One study compared embryonic pnc development of the six *Geospiza* finch species and analyzed expression patterns of candidate growth factor genes involved in avian craniofacial development (Abzhanov et al., 2004). This study found a correlation between earlier and spatially broader expression of *Bone morphogenetic protein 4* (*Bmp4*) in the developing upper beak and the deep, wide beak morphology of the ground finches (Abzhanov et al., 2004). *Bmp4*, however, was not implicated in the alternative elongated beak phenotype, suggesting the involvement of other genes (Abzhanov et al., 2006). To investigate the genetics of beak elongation, and go beyond candidate genes with a known role in craniofacial development, Abzhanov et al. (2006) subsequently used a DNA microarray analysis. Using the sharp-beaked finch *G. difficilis* as a reference, transcripts up-regulated in the long-beaked cactus finches were distinguished from transcripts that were down-regulated or whose expression remained unchanged in the ground finches (Abzhanov et al., 2006). This approach revealed *Calmodulin* (*CaM*), a Ca^{2+} binding protein involved in Ca^{2+}-dependent signal transduction, as a top candidate for beak morphogenesis. Further experiments misexpressing *CaM* in chick embryos produced the expected elongated beak phenotype

(Abzhanov et al., 2006). Together, these studies suggested a modular developmental genetic basis for variation in pnc-determined beak morphology in which *Bmp4* regulates depth and width, and *CaM* acts on the length axis. A complementary study that focused on pmx development in the ground finches used the same microarray screen to reveal three candidate genes for pmx patterning: *TGFβ receptor type II* (*TGFβIIr*), *β-catenin*, and *Dickkopf-3* (*Dkk3*) (Mallarino et al., 2011). Further analysis showed that domains of expression of these candidate genes correlated with adult morphology and that the genes interact to determine different axes of growth (Mallarino et al., 2011).

Prior to Lamichhaney et al.'s (2015) comprehensive genomic analysis, two Darwin's finch genomes had been sequenced. In 2012, the genome of a female medium ground finch, *Geospiza fortis* was published (Zhang et al., 2012) as part of a suite of avian genomes (Jarvis et al., 2015; Zhang et al., 2014a; Zhang et al., 2014b). In 2013, Rands et al. (2013) published the genome of *G. magnirostris* and analyzed it in comparison to other vertebrates; zebra finch and *G. fortis* in particular. An analysis of positive selection by Rands et al. (2013), based on patterns of synonymous and non-synonymous substitutions in a filtered set of 1,452 orthologs, yielded 21 genes with putatively adaptive amino acid substitution in the Darwin's finch lineage. At least two of these genes, *POU1F1 and IGF2R*, have been implicated in craniofacial development, suggesting a potential role in beak morphogenesis.

1.5 Integrating genomics of adaptive radiation and field biology

In the latest advance in this historic tale, Lamichhaney et al. (2015) present an expanded genomic approach to understanding the evolutionary history of Darwin's finches. They sequence 120 full genomes, representing all the species in the Darwin's finch radiation and incorporating

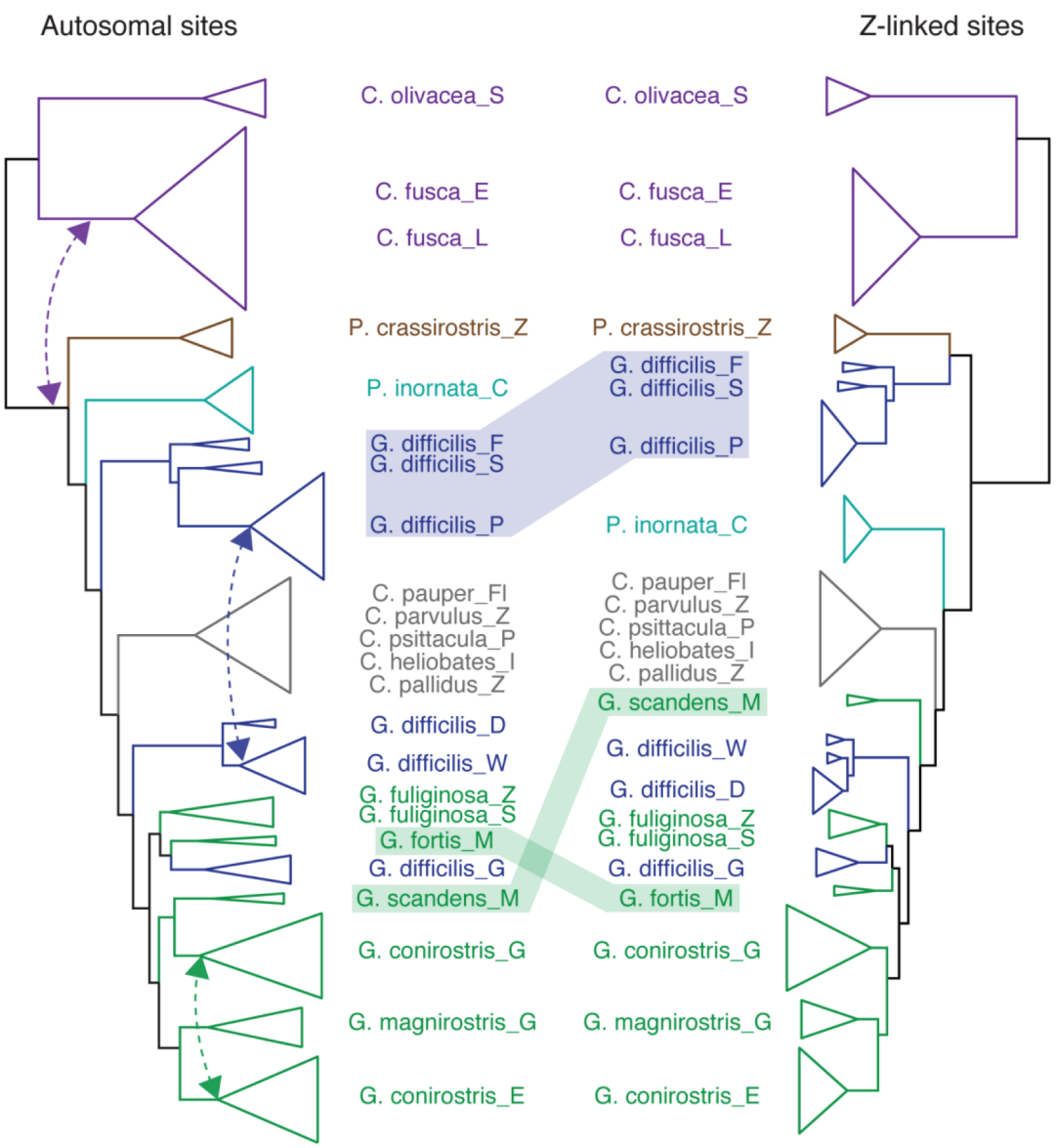

Figure 2 | Maximum-likelihood phylogenies of Darwin's finches. Dashed arrows indicate gene flow between species. Highlighted bars denote key discordances between the trees. Branches ending with triangles indicate multiple genomes. Letters after species names indicate island sampled: S: Santiago, E: Española, L: San Cristóbal, Z: Santa Cruz, F: Fernandina, C: Cocos, P: Pinta, Fl: Floreana, I: Isabela, M: Daphne, D: Darwin, W: Wolf, G: Genovesa.

populations from multiple islands, and two closely related tanagers, *Tiaris bicolor* and *Loxigilla noctis*. Analysis of this dataset reveals some striking patterns. First, in concordance with prior observations reporting interspecies hybridization and migration between islands, whole-genome comparisons between species reveal high genetic diversity and extensive sharing of genetic variation, especially between ground and tree finches. The autosomal genome-based phylogenetic tree dates the birth of the radiation to circa 900,000 years ago and the radiation of ground and tree finches to 100,000-300,000 years ago. This tree topology generally supports the classical taxonomy based on mtDNA and morphology (Farrington et al., 2014; Lack, 1947; Petren et al., 2005), with warbler finches as the first group to branch off and the ground and tree finches as the crown group. However, the phylogeny reveals two polyphyletic species, *G. difficilis* (also reported in Farrington et al., 2014) and *G. conirostris*, which depart from the existing taxonomy. *G. difficilis*, which occurs on six islands, is split into three groups, and *G. conirostris* is split into two groups (Figure 2). The polyphyletic groupings of both species are associated with taxon sampling from multiple islands, emphasizing the importance of geography in the branching order of recently evolved groups.

Lamichhaney et al. attribute allele sharing between species to introgressive hybridization via multiple lines of evidence, including ABBA-BABA tests (Durand et al., 2011; Green et al., 2010) and discordance between autosomal and sex-linked phylogenetic tree topologies (Figure 2). ABBA-BABA tests show that despite a closer genetic relationship to *G. magnirostris* on Genovesa, *G. difficilis* on Wolf shares alleles with *G. difficilis* on Pinta. Another ABBA-BABA comparison confirms the proximate genetic relationship of *G. magnirostris* on Genovesa and *G. conirostris* on Española, but also shows gene flow between *G. conirostris* on Española and *G. conirostris* on Genovesa. Introgression of loci affecting phenotypic characters could explain the

similarities upon which the two *G. difficilis* populations and the two *G. conirostris* populations were grouped in the classical taxonomy. In addition to these cases of recent introgressive hybridization, the authors find ABBA-BABA support for gene flow between the warbler finch *C. fusca* and the common ancestor of the non-warbler finches. Sex-linked genes are well known to play a large role in speciation, and hence these loci generally show less interspecific gene flow in comparison to autosomal loci (Qvarnström and Bailey, 2009). The discordance between the autosomal and sex-linked tree topologies for Darwin's finches, particularly with respect to the placement of *G. difficilis* from Pinta, Fernandina, and Santiago, supports the hypothesis of gene flow between this group and the ground and tree finches after the split of the Cocos finch. Phylogenies based on mtDNA and W-linked loci also support this interpretation. In addition, a separate analysis of demographic history within the group shows a large effective population size among the ground finches in comparison to the other taxa, consistent with gene flow among ground finch species.

To explore the genetic architecture of beak shape variation, Lamichhaney et al. perform a genome-wide scan of genetic differentiation (ZF_{ST}) on 15-kilobase (kb) windows between two groups of closely related finches distinguished by having blunt (*G. magnirostris* from Genovesa and *G. conirostris* from Española) or pointed (*G. conirostris* from Genovesa and *G. difficilis* from Wolf) beaks. A number of genomic regions emerge from this analysis, many of which house genes with potential roles in beak development. The highest-scoring window contains the gene *ALX homeobox 1* (*ALX1*), which is known to play a central role in vertebrate craniofacial development (Dee et al., 2013; Uz et al., 2010). A phylogenetic tree of Darwin's finches based on the *ALX1* region groups individuals into two clades based on their blunt versus pointed beak morphology (Figure 3). The divergence between blunt and pointed haplotypes is inferred to be

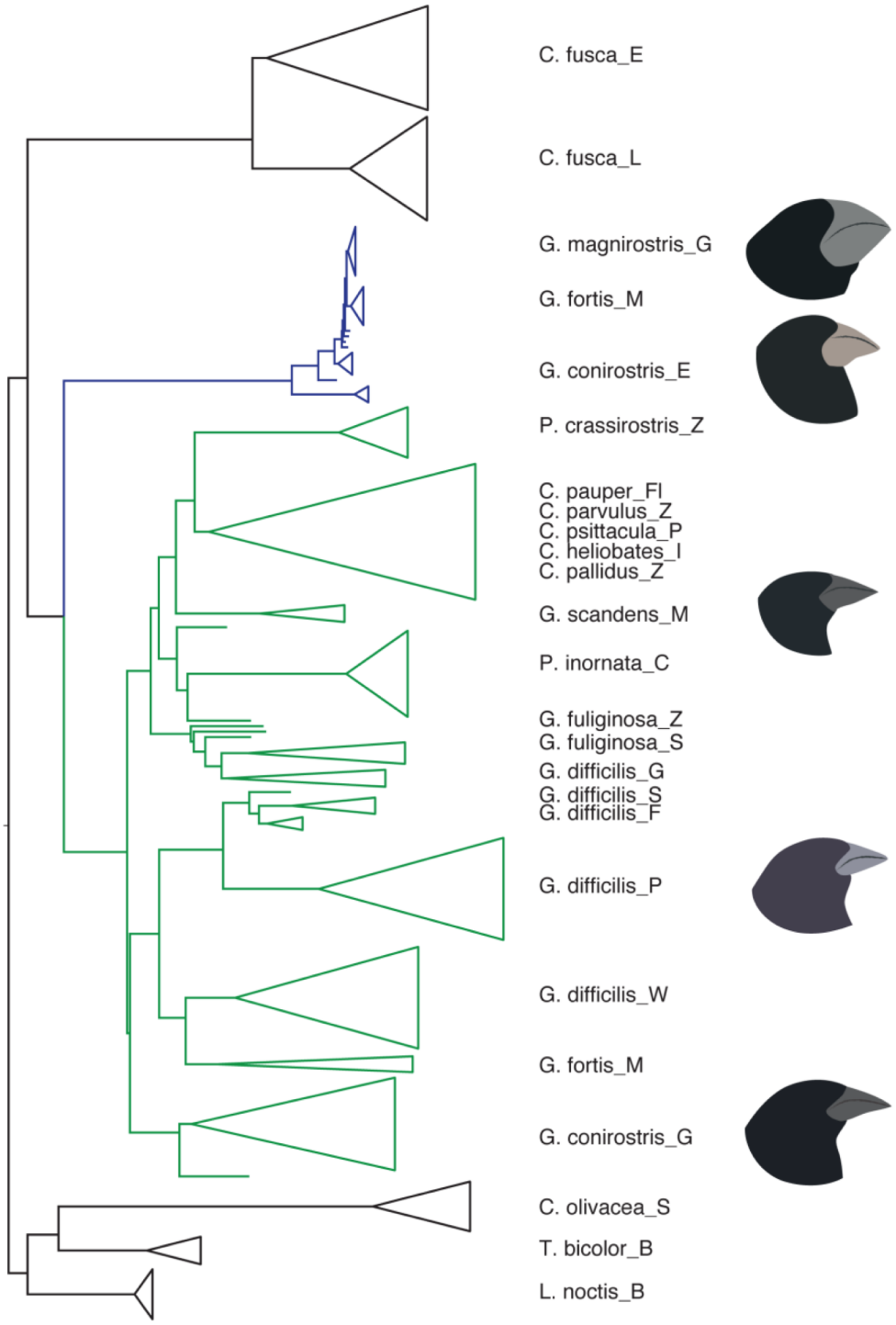

Figure 3 | Haplotype tree of beak shape locus *ALX1*. Neighbor-joining tree based on *ALX1* reveals a deep split between blunt and pointed beak haplotypes. Representative finch heads reflect species grouping by beak morphology as opposed to historical branching order. Branches ending with triangles indicate multiple *ALX1* haplotype sequences.

quite old, having occurred soon after the split of the warbler finches and other Darwin's finches. The medium ground finch, *G. fortis*, a species that varies in beak shape on Daphne Major, is also polymorphic for these highly divergent *ALX1* haplotypes, and SNP genotyping of *G. fortis* specimens from this island reveals a significant association between the *ALX1* locus and blunt versus pointed beak morphology.

1.6 Introgression and adaptation

Genomic studies in various systems have uncovered evidence for adaptive allele sharing between closely related species, apparently as a result of introgression (Poelstra et al., 2014; Ellegren et al., 2012; Martin et al., 2015; Joyce et al., 2011; Prüfer et al., 2014; Vernot and Akey, 2014; Rieseberg et al., 2003; Abbott et al., 2013), and several of these investigations point to the exchange of distinct phenotypic traits (Figure 4). For instance, mosquitoes in the *Anopheles gambiae* complex have experienced such extensive interspecific gene flow that most of the genome no longer reflects the history of species-level diversification (Fontaine et al., 2015), and traits such as desiccation resistance and insecticide resistance have been transferred between species as a result (Norris et al., 2015; Fouet et al., 2012; Gray et al., 2009). Similarly, the house mouse, *Mus musculus domesticus,* has experienced substantial gene flow from the Algerian mouse, *Mus spretus* [20], resulting in introgression of alleles at olfactory receptors (Liu et al., 2015) as well as rodenticide resistance (Song et al., 2011). *Heliconius* butterflies have a long history of divergence with gene flow (Martin et al., 2013) and haplotypes at two major loci controlling wing patterning have been transferred among groups of closely related species as a result of natural selection for mimicry (Heliconius Genome Consortium, 2012; Pardo-Diaz et al., 2012). Even modern humans have benefited from introgression: a haplotype at the hypoxia

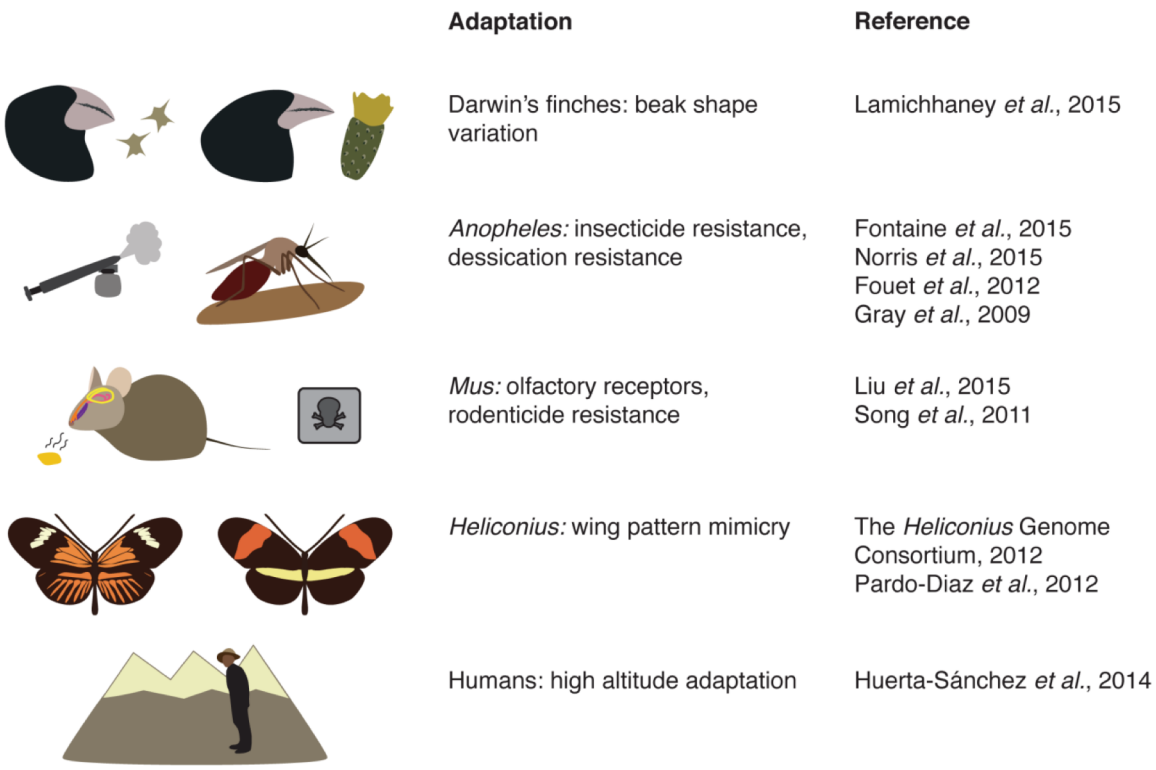

Figure 4 | Summary of recent studies of adaptive introgression in animals. Examples highlight the exchange of distinct adaptive phenotypic traits between species.

pathway gene *EPAS1*, associated with high-altitude hemoglobin concentration in Tibetans, appears to have been acquired from a Denisovan-like archaic human lineage (Huerta-Sanchez et al., 2014).

It is important to note, however, that two distinct evolutionary processes can produce similar patterns of shared ancestry at focal regions of the genome: introgression and incomplete lineage sorting (ILS) of ancestral variation. For instance, in the case of the finches, it is possible that because the blunt and pointed *ALX1* haplotypes diverged long ago, prior to much of the species-level diversification, this may be a long-standing polymorphism that has sorted out over time, resulting in some species becoming fixed for one ancient haplotype (blunt) and other

species becoming fixed for the other ancient haplotype (pointed). Under this scenario, species share similar sequences today and group by phenotype on the *ALX1* tree as a result of ILS, not introgression. Work in *Anopheles* (Fontaine et al., 2015), *Mus* (Liu et al., 2015), *Heliconius* (Smith and Kronforst, 2013), and humans (Huerta-Sanchez et al., 2014) has explicitly considered ILS as an alternative explanation to introgression at target loci and the data from these systems generally support the introgression hypothesis. Overall, Lamichhaney et al. present compelling genome-wide evidence for a history of divergence with gene flow among Darwin's finches and remarkable allele sharing at a locus responsible for phenotypic diversity and adaptation. In terms of *ALX1* specifically, some patterns in the data, such as the very short branch lengths among blunt haplotype sequences on the *ALX1* tree, are definitely consistent with introgression (and selection). In contrast, the relatively long branch lengths among pointed haplotype sequences, and the fact that the *G. fortis* sequences do not group with *G. scandens* and *G. fuliginosa*, putative donor species (Lamichhaney et al., 2015), may suggest a potential role for ancestral variation as well. Future work including expanded sampling and sequencing of *G. fortis* from Daphne Major, and analyses of DNA sequence divergence and ABBA-BABA patterns of allele sharing among putatively introgressed *ALX1* haplotypes will help clarify this history.

1.7 Conclusions and outlook

Lamichhaney et al.'s discovery of *ALX1* raises many fascinating questions. For instance, what is the ultimate source of the two highly divergent, blunt and pointed haplotypes? The authors detect a genome-wide signature of ancient introgression between *C. fusca* and the common ancestor of the non-warbler finches, which may indicate that ancient hybridization contributed some of the critical genetic variation - perhaps one of these *ALX1* haplotypes even - that originally fueled the

finch radiation on the Galápagos. Furthermore, Lamichhaney et al. present evidence that these two haplotypes frequently occur together in heterozygotes, both in interspecific hybrids and in polymorphic species such as *G. fortis*. However, based on the sequence data presented, the two haplotypes do not appear to recombine. This may suggest that structural variation, like a chromosomal inversion polymorphism, is maintaining alternate copies. By reducing recombination between loci, inversions can maintain linkage between co-adapted alleles and this can have profound impacts on adaptation and speciation (Kirkpatrick and Barton, 2006; Joron et al., 2011; Kunte, Zhang et al., 2014). Moving beyond *ALX1*, it will be fascinating to explore the evolution of the many other genes that emerged from the genome-wide comparison between finches with blunt and pointed beaks. Given that birds with differing beak morphology are also likely to differ in other aspects of their biology, a detailed analysis of these genes and their evolutionary histories is almost certain to yield insights far beyond beak development.

Finally, we must note that it is not only the incredible dataset, sophisticated analyses, and discovery of *ALX1* that make this most recent study of Darwin's finches so remarkable, but the integration of these new insights with detailed knowledge collected over decades about the ecology and evolutionary history of the study system. Genome sequencing technology will continue to advance and the application of these tools will proceed virtually without limit, but the biological context in which we interpret these genomic data is irreplaceable. In our modern exploration of evolutionary biology, natural history and ecology are essential counterparts to genomics because they enable us to establish direct connections between sequence variation and natural selection. For this reason, Darwin's finches have been providing critical insight into the evolutionary process for over 150 years and it seems that they still have plenty more to tell us.

2 Experimental field tests of Batesian mimicry in the swallowtail butterfly *Papilio polytes*[2]

2.1 Abstract

The swallowtail butterfly *Papilio polytes* is known for its striking resemblance in wing pattern to the toxic butterfly *Pachliopta aristolochiae*, and is a focal system for the study of mimicry evolution. *P. polytes* females are polymorphic in wing pattern, with mimetic and non-mimetic forms, while males are monomorphic and non-mimetic. Past work invokes selection for mimicry as the driving force behind wing pattern evolution in *P. polytes*. However, the mimetic relationship between *P. polytes* and *P. aristolochiae* is not well understood. In order to test the mimicry hypothesis, we constructed paper replicas of mimetic and non-mimetic *P. polytes* and *P. aristolochiae*, placed them in their natural habitat, and measured bird predation on replicas. In initial trials with stationary replicas and plasticine bodies overall predation was low and we found no differences in predation between replica types. In later trials with replicas mounted on springs and with live mealworms standing in for the butterfly's body we found less predation on mimetic *P. polytes* replicas compared to non-mimetic *P. polytes* replicas, consistent with the predator avoidance benefits of mimicry. While our results are mixed, they generally lend support to the mimicry hypothesis as well as the idea that behavioral differences between the sexes contributed to the evolution of sexually dimorphic mimicry.

[2] A version of this chapter has been published as: Palmer DH, Tan YQ, Finkbeiner SD, Briscoe AD, Monteiro A and MR Kronforst. 2018. Experimental field tests of Batesian mimicry in the swallowtail butterfly *Papilio polytes*. Ecology and Evolution. In press.

2.2 Introduction

Mimicry is a classic example of evolution by natural selection. H.W. Bates (1862) noted the resemblance between sympatric but distantly related butterfly species, some of which were unpalatable to predators and some of which were palatable. Bates posited that if predators sampled the unpalatable species first they would subsequently avoid this species and its palatable mimic. Batesian mimicry thus relies on the interactions between the warning signal of the unpalatable species, the predators that avoid the warning signal, and the mimic's ability to dupe the predator by emulating the warning signal (Ruxton et al., 2004).

How predators perceive and respond to warning phenotypes are consequential questions for understanding how natural selection shapes mimetic adaptations. Batesian mimicry is known to occur across animals and plants through different sensory modalities, but visual signals are the best known and understood (Cott, 1940). Visual mimicry signals include changes in coloration, body structure, and behavior, and these often function in concert to achieve integrated mimetic phenotypes (Wickler, 1968). Birds are a major predator class across invertebrate and vertebrate Batesian mimicry systems (Cott, 1940; Wickler, 1968), and have become models for studying predator psychology and visual physiology. Depending on the mimicry system, birds can learn to avoid mimetic phenotypes, (Gittleman and Harvey, 1980; Roper and Redston, 1987; Guilford, 1990; Endler, 1991), or may evolve innate avoidance if models are harmful enough (Smith, 1975; Smith, 1977; Schuler and Hesse, 1985).

Papilio polytes is a female-limited polymorphic mimic distributed widely throughout Southeast Asia; males have a single non-mimetic phenotype and females have either a male-like non-mimetic form or one of three mimetic forms that each resembles a distinct toxic *Pachliopta* swallowtail. A rich body of theory and experimental work addressing the evolutionary genetics

of mimicry and mate choice preferences has emerged from this system (Fryer, 1914; Clarke and Sheppard, 1972; Ohsaki, 1995; Uesugi, 1996; Kitamura and Imafuku, 2010; Nishikawa et al., 2013; Kitamura and Imafuku, 2015; Low and Monteiro, 2018) including the discovery of *doublesex* as the genetic locus controlling mimetic polymorphism in *P. polytes* (Kunte, Zhang et al., 2014; Nishikawa et al., 2015). While this work has clarified the molecular underpinnings of *P. polytes* and *Pachliopta* mimicry, less has been done experimentally to examine the ecological consequences associated with the mimetic relationship itself.

Mimicry in *P. polytes* was first reported by naturalists who noted the similarity in wing patterns between morphs of *P. polytes* and two *Pachliopta* species (Wallace, 1865; Fryer, 1913). Clarke and Sheppard (1972) later found correlations between the ranges of different mimetic morphs and their putative corresponding models across Southeast Asia. Ohsaki (1995) examined beak marks on the wings of wild caught *P. polytes* and *Pachliopta artistolochiae* as a proxy for bird predation. His analysis reported comparable beak mark percentages (28-29%) on the toxic *P. aristolochiae* and the mimetic form of *P. polytes* that matches the *P. aristolochiae* wing pattern. In contrast, Ohsaki found an elevated percentage of beak marks (53%) on non-mimetic *P. polytes*, suggesting that non-mimetic *P. polytes* experienced more predation than mimetic *P. polytes* females. Uesugi (1996) conducted feeding trials with seven wild-caught birds (*Hypsipites amaurotis*) in a lab setting and found that after an initial training session where birds were fed *P. aristolochiae* the birds reduced their consumption of mimetic *P. polytes*, consistent with a learned aversion to the wing pattern. Additionally, analyses of flight kinematics suggest that mimicry extends beyond wing patterning to behavioral similarity between *P. polytes* and *P. aristolochiae* in wing movements and flight path (Kitamura and Imafuku, 2010; Kitamura and Imafuku, 2015). Taken together, these studies are highly suggestive of an adaptive resemblance

between mimetic *P. polytes* and *P. aristolochiae* resulting in predator avoidance, but there exist no direct tests of Batesian mimicry using natural populations of these species and free-ranging bird predators.

Replicas of naturally occurring prey have been used to measure predator-mediated natural selection in diverse taxa, including insects (Lövei and Ferrante, 2017), fish (Caley and Schluter, 2003), frogs (Saporito et al., 2007), salamanders (Kuchta et al., 2005), lizards (Stuart-Fox et al., 2003), snakes (Pfennig et al., 2001), turtles (Marchand et al., 2002), birds (Ibáñez-Álamo et al., 2015), and mice (Vignieri et al., 2010). These experiments allow for precise manipulation of artificial models in order to test specific hypotheses about how mimicry phenotypes, or parts thereof, may experience differential predation. The artificial prey method has been implemented in diverse butterfly systems to address the relationship between wing patterning and predation (Finkbeiner et al., 2012; Merrill et al., 2012; Finkbeiner et al., 2014; Seymoure and Aiello 2015; Dell'Aglio et al., 2016; Ho et al., 2016; Finkbeiner et al., 2017a,b; Wee and Monteiro, 2017). In this study, we applied the artificial prey method to study how female-limited Batesian mimicry operates in wild populations. We constructed replicas of *P. polytes* morphs and *P. aristolochiae,* with realistic color patterns and reflectance, and exposed them to natural predators in the field. We directly assayed bird predation rates based on attack marks or the loss of a bait, and tested for differential predation among the sexes and morphs of *P. polytes* in comparison to *P. aristolochiae* in order to analyze the selective advantage of mimicry.

2.3 Materials and Methods

We conducted two complementary predation experiments to address different aspects of mimicry in the field. In the first phase, we deployed a large number of stationary artificial prey of four

different phenotypes to assay the role of wing patterning alone. Phase I replicas were deployed in an open wing basking position. In the second phase, we used fewer artificial prey types but incorporated biologically meaningful features like butterfly replica movement and a live bait providing body movement and odor to make the trials more realistic. Phase II replicas used a closed wing resting position.

2.3.1 Phase I

2.3.1.1 Paper replica construction

We constructed 4 artificial prey types: mimetic *Papilio polytes* female, non-mimetic *P. polytes* female, *P. polytes* male (which are always non-mimetic), and *Pachliopta aristolochiae* (Figure 5). *P. aristolochiae* represents the toxic, unpalatable model in this mimicry system whereas the *Papilio* morphs are non-toxic, palatable species. Although *P. polytes* has multiple mimetic forms across its range, we built our replicas based on the local mimetic morph found in Singapore where all experimental trials were conducted. Similarly, we based our *P. aristolochiae* replicas on the local morph that *P. polytes* mimics. Artificial butterfly replicas were designed following methods described in Finkbeiner et al. (2012), where natural butterfly wings were referenced to create spectrally matched paper wings. We first generated digital images of each replica type's wing pattern in Adobe Illustrator and then printed the wings on low-reflective Whatman qualitative filter paper (No. 1001-917), using an Epson Stylus Pro 4880 printer with UltraChrome K3 ink. We applied Crayola® crayon (Gel FX yellow) over the white/yellow hindwing patches of the printed wings where reflectance properties were difficult to reproduce with printed colors alone. We cut out the printed wings with a laser cutter and affixed them to

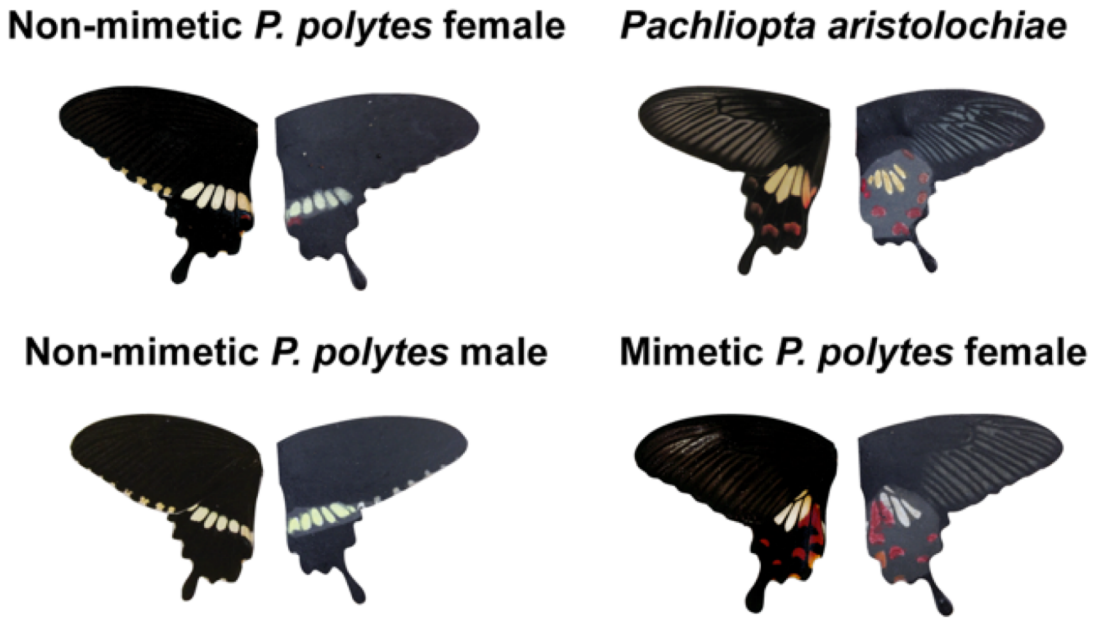

Figure 5 | Hypothesized Batesian mimicry between *Papilio polytes* and *Pachliopta aristolochiae*. For each panel, left depicts real wing, right depicts Phase I wing replica.

black cardstock backings. To increase the replicas' durability in the field we dipped the non-chromatic (black/gray) portions of the replicas in molten paraffin wax. Finally, we attached plasticine abdomens (Newplast®) to capture the imprints left by predators. The three *Papilio* replica types were given black abdomens and the *Pachliopta* replicas had half black, half red abdomens to emulate the abdomens of real *Pachliopta*.

To evaluate the similarity between real butterflies and our constructed replicas we measured the reflectance spectra of real butterfly wings and abdomens, and artificial butterfly wings (after the molten wax treatment) and abdomens using an Ocean Optics USB2000 fiber optic spectrometer, with a bifurcating fiber cable (R400-7-UV-vis, Ocean Optics) connected to a deuterium-halogen tungsten lamp (DH-2000, Ocean Optics). We used a white spectralon

standard (WS-1-SL, Labsphere) during calibration, and placed the detecting fiber in a probe holder at a 45° angle to the plane of the butterfly wing. We designed butterfly replicas to resemble butterflies basking with wings open, and therefore only utilized the dorsal side.

2.3.1.2 Predation tests

All experimental data were collected in Singapore between June and July 2014. The three field sites were Kent Ridge Park, MacRitchie Reservoir, and Pulau Ubin. A total of 192 paper replicas were tested at Kent Ridge Park, 384 were tested at MacRitchie Reservoir, and 1216 were tested at Pulau Ubin due to size differences in the available area of the field sites. Kent Ridge Park and Pulau Ubin both contain fragmented forest, and MacRitchie Reservoir contains mature forest. Jain et al. (2017) reported relative abundances of *P. artistolochiae* to *P. polytes* of approximately 1:10 for fragmented forest and 1:17 for mature forest. Replicas were placed in the field in sets of 16 individuals (4 of each type), with at least a 2 m distance between individual paper butterflies. These were attached to plants at a height of approximately 1.5 m with either thread or Blu-Tack. Each set of 16 was spaced at least 200 m apart from the next to reduce the effects of predator learning on predation attempts, and each set locality was only used once. Replicas remained in place for 4 days and were examined every day for predation marks. Attacks were recorded when beak marks were found imprinted on the plasticine body (Figure 6a-c). Other markings on the plasticine such as insect mandibular imprints were not counted in these attacks. To analyze attack data, we used a generalized linear model (GZLM) with a binomial distribution (replica attacked or not), and replica type and site identity as fixed effects.

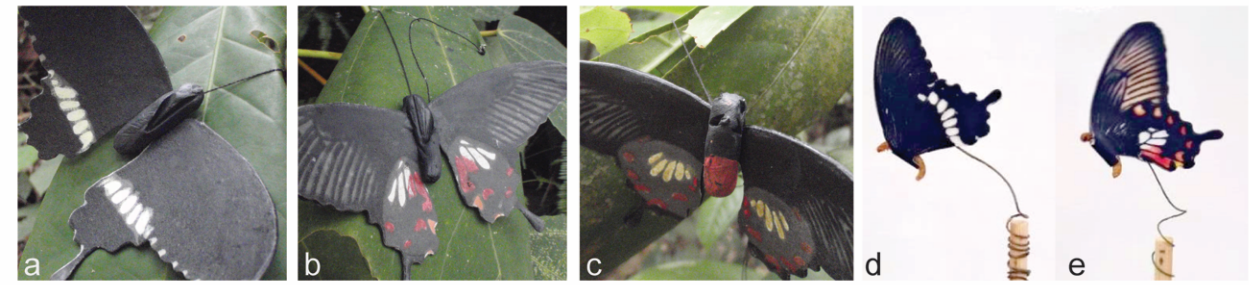

Figure 6 | Fully assembled butterfly replicas. a-c: Phase I replicas showing bird beak marks on the plasticine bodies. d-e: Phase II replicas with mealworm bodies mounted on wooden sticks.

2.3.2 Phase II

2.3.2.1 Selection of field sites

Four new field sites were identified, Jurong Eco Garden, Medicinal Garden at Khoo Teck Puat Hospital, North Buona Vista Road, Singapore (01°29' N, 103°78' E) and the degrading secondary forest along Upper Aljunied Road (01°34' N, 103°87' E), in order to avoid repeated interactions with predators involved in previous trials. All sites consist of fragmented forest, but the North Buona Vista Road site and Upper Aljunied Road sites were reported to have no *P. aristolochiae* sightings nor *P. aristolochiae* host plants (personal communication). We conducted preliminary trials at the new sites to ensure that birds were actively seeking prey at these locales. We constructed paper replicas of *Mycalesis perseus*, a common, palatable species in Singapore (Ho et al., 2016) and placed 10 replicas in 2 m intervals at each site. A site was considered to experience active predation if 50% of the replicas were attacked within two days. All four new sites (JEG, KTPH, NBVR, UAR) fulfilled this condition and were used in subsequent trials.

2.3.2.2 Paper replica construction

We constructed 2 new artificial prey types to resemble mimetic and non-mimetic *P. polytes* with their wings closed, showing only their ventral wing surfaces. We generated digital images of these wings using a Leica DMS1000 and Adobe Photoshop CS6. The wing images were printed on Daler-Rowney 95gsm A4 Sketch Paper using a Samsung Laser Jet 500 Colour M551 printer. The printed white patches were colored using a Derwent Studio Chinese White 72 color pencil to more closely match the real specimens. We treated the non-printed side of the wings with colorless paraffin wax to waterproof them and capture potential beak imprints without altering the printed colors. Reflectance spectra were taken from ventral wing surfaces of the real *P. polytes* and from the printed replicas using an Ocean Optics USB2000 spectrometer and using a light probe placed at 90° to the sample. One live mealworm (*Tenebrio molitor* larva) was secured to each pair of wings using Faber-Castell Tack-It and these were mounted on wooden sticks using green floral wire (Fig 2d-e). We coiled the mounting wire to enable wind-driven movement of the replicas. The base of each wooden stick was coated with a water-based insect repellent to deter unwanted (non-avian) predators.

2.3.2.3 Predation tests

At each of the sites (JEG, KTPH, NBVR, UAR) we set out 3 groups of 10 *P. polytes* replicas (5 mimetic and 5 non-mimetic). Within each group, alternating mimics and non-mimics were planted in the ground at a height of 25-30 cm, approximately 2 m apart from one another. Replicas remained at the site for 2 days for each trial. These were inspected daily and predation was recorded when the mealworm was removed or damaged or when bite marks were present on

the wings. We used a GZLM with a binomial distribution, and replica type and site identity as fixed effects to analyze differences in predation.

2.3.3 Discriminability tests

We calculated discriminability using a bird vision model to verify that our paper replicas accurately resembled their real counterparts through the eyes of avian predators. A number of insectivorous birds inhabit Singapore (Castelletta et al., 2005), but the specific predators of *P. polytes* in this area are unknown. For each replica type, we compared color patches (white, black, and red if present) between real specimens and paper replicas and calculated their similarity in units of just noticeable differences (JNDs) using the receptor-noise model of Vorobyev and Osorio (1998). The comparisons were made using the blue tit (*Cyanistes caeruleus*) cone sensitivities, which represent the UV-type avian visual system. We followed the work of Hart et al. (2000) including the effects of blue tit ocular media and used a Weber fraction=0.05 and relative abundances of cones (UV=0.37, S=0.7, M=0.99, L=1). We analyzed replicas from Phase I using low light intensity and Endler's (1993) forest shade irradiance spectra because they were placed in the forest understory. For Phase II replicas we used low light intensity and Endler's (1993) daylight irradiance spectra because these models were placed in open areas. Low light intensity conditions were selected for both Phase I and Phase II as a more ecologically relevant prediction: avian predators are most active during morning hours when natural light is less bright, and previous work in the tropics has shown experimental evidence that avian attacks on artificial butterfly models occur almost exclusively during the early morning (Finkbeiner et al. 2012).

2.4 Results

2.4.1 Discriminability tests

The spectral comparisons between color patches of real specimens and paper replicas are presented in Figure 7, showing that the reflectance spectra are generally concordant between the real specimens and replicas. The avian vision modeling results showed that 17 out of 20 color patch comparisons had JND values below the discriminability threshold of 1.0, and were thus considered indiscriminable to birds, while the other 3 comparisons still had low JND values between 1.0 and 1.3.

2.4.2 Phase I

A total of 1792 individual paper replicas were tested among the three sites (192 at Kent Ridge Park, 384 at MacRitchie Reservoir, and 1216 at Pulau Ubin). We observed a variety of markings on the plasticine bodies of the replicas including imprints from bird beaks (Figure 6a-c), arthropod mandibles, and from one small reptile or mammal. Across the 4 types we calculated an overall avian predation rate of 1.9%. Cases where the paper replicas could not be found at the end of the test period were excluded from the data set.

Avian predation results for Phase I are summarized in Table 1. While we did find a larger number of attacks on non-mimetic female *P. polytes* compared to mimetic *P. polytes,* consistent with the expectations of Batesian mimicry, we also found that *P. aristolochiae* replicas experienced the most attacks and non-mimetic males the fewest attacks. Results from our generalized linear model showed that replica type was not a significant predictor of attack number, but site identity was a significant predictor (Table 2). A subsequent model including

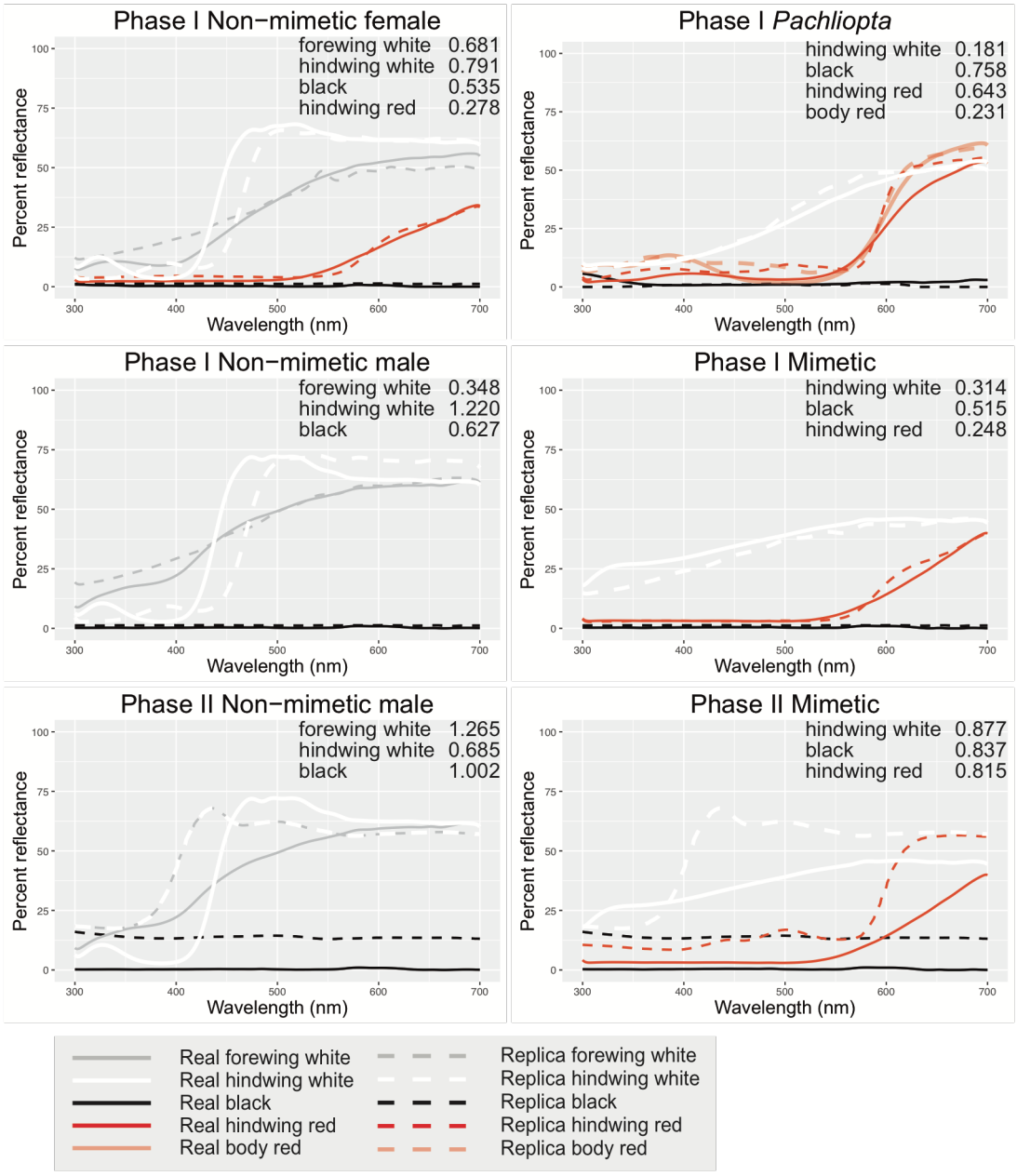

Figure 7 | Reflectance spectra of real and replica color patches, and results of discriminability modeling of the UV-type avian visual system. Percent reflectance for each color patch is shown from 300nm-700nm, which is the avian visual range. Avian vision modeling results for each color patch are in units of just noticeable differences (JNDs).

only site identity as a fixed effect showed that replicas at the Pulau Ubin site experienced significantly less predation than Kent Ridge Park or MacRitchie Reservoir (Table 2).

Table 1 | Avian predation in Phase I experiments

	P. polytes Non-mimetic female	*P. polytes* Non-mimetic male	*P. polytes* Mimetic	*Pachliopta aristolochiae*
Kent Ridge Park	3 (46)	1 (47)	1 (48)	3 (45)
MacRitchie Reservoir Park	3 (90)	2 (90)	1 (87)	5 (83)
Pulau Ubin	3 (279)	1 (276)	4 (274)	5 (278)
Total	9 (415)	4 (413)	6 (409)	13 (406)

* Number attacked (number not attacked)

Table 2 | Results of generalized linear model for Phase I experiments

Model	Estimate	Std. error	z-value	p-value	df
Predation ~ replica type + site identity					
Replica type	0.2075	0.1629	1.273	0.202854	1791
Site identity	-0.7213	0.2156	-3.345	0.000822	1791
Predation ~ site identity					
Kent Ridge Park v MacRitchie Reservoir	-0.3882	0.4733	-0.820	0.41213	1791
Kent Ridge Park v Pulau Ubin	-1.3921	0.4563	-3.051	0.00228	1791
MacRitchie Reservoir v Pulau Ubin	1.0039	0.4139	2.425	0.01529	1791

2.4.3 Phase II

A total of 120 individual paper replicas (mimetic and non-mimetic *P. polytes*) were tested among the four sites (15 mimetic and 15 non-mimetic at each site). Predation results for Phase II are summarized in Table 3. We again tested for differential predation between mimetic and non-mimetic types. At each site mimics experienced fewer predation events than non-mimics, and all attacks combined showed approximately 30% less predation on mimics than non-mimics. However, the p-value for replica type was slightly above the statistical significance cutoff of 0.05 (Table 4). Predation was not significantly different between sites in Phase II (Table 4).

Table 3 | Avian predation in Phase II experiments

	P. polytes Non-mimetic	*P. polytes* Mimetic
Jurong Eco Garden	8 (7)	5 (10)
Khoo Teck Puat Hospital	9 (6)	6 (9)
North Buona Vista Road	8 (7)	5 (10)
Upper Aljunied Road	9 (6)	8 (7)
Total	34 (26)	24 (36)

* Number attacked (number not attacked)

Table 4 | Results of generalized linear model for Phase II experiments

Model	Estimate	Std. error	z-value	p-value	df
Predation ~ replica type + site identity					
Replica type	-0.67768	0.37175	-1.823	0.0683	119
Site identity	0.13775	0.16653	0.827	0.4081	119

2.5 Discussion

We generated realistic artificial prey and tested for mimetic protection from predation in *P. polytes*. In Phase I we observed generally low attack rates and did not find significant differences in predation between mimetic and non-mimetic *P. polytes*. In Phase II we observed the expected lower levels of predation on mimetic replicas compared to non-mimetic replicas at individual sites, but these were not statistically significant overall and fell just slightly above the significance value of 0.05. These results suggest that mimetic morphs of *P. polytes* experience a selective advantage over non-mimetic *P. polytes* by deterring predators, consistent with the basic predictions of Batesian mimicry.

Trials in Phase I resulted in significantly lower predation rates in comparison to Phase II (1.91% and 48.33% respectively; chi-squared= 497.01, df=1, $p<0.001$). Phase I predation rates were also lower than those reported in other butterfly predation studies using similar methods (6.38% in Finkbeiner et al., 2012; 54.4% in Ho et al., 2016; 51% in Wee and Monteiro, 2017). Replicas in Phase I were fixed to leaves and remained stationary while those in Phase II were mounted on springs that allowed for movement and also incorporated a live bait. It is possible that the immobile conditions of Phase I made the artificial prey difficult for predators to visually detect. Other possible explanations for differences in predation rates between field sites might include the availability of alternative prey, frequency of models to mimics, predator abundance, and/or predator/prey seasonality (Finkbeiner et al., 2018).

In Phase II we observed slightly increased attacks on non-mimetic morphs compared to mimetic morphs at each individual site that just missed the p-value significance cutoff of 0.05, when analyzed using a GZLM. This result suggests a modest benefit to mimetic individuals of

this species, and with higher power and a larger sample size, a significant difference in predation is expected between these two species. More trials need to be conducted to explore this question. The black reflectance values in Phase II replicas were brighter than in Phase I, possibly making the Phase II replicas more detectable to predators and thus more likely to be attacked overall. Although Phase I replicas more closely resembled their real counterparts than Phase II replicas (Phase I had lower JNDs overall), Phase II replicas elicited predation differences in the direction expected under Batesian mimicry.

Behavioral differences between the sexes have long been hypothesized to drive the evolution of female-limited mimicry. Wallace (1865) proposed that female butterflies experience more predation than their male counterparts when searching for host plants while laden with eggs and while hovering over plants during oviposition. The evolution of flight mimicry in *P. polytes* supports this idea; wing beat and flight path are significantly different between mimetic and non-mimetic individuals, and mimetic individuals fly like the toxic *Pachliopta aristolochiae* model (Kitamura and Imafuku, 2010; Kitamura and Imafuku, 2015). Ohsaki (1995) proposed that females disproportionately benefit from evolving mimicry and indeed found that wild-caught non-mimetic *P. polytes* females had nearly double the proportion of beak marks on their wings compared to *P. polytes* males (which are always non-mimetic). More recently, Su et al. (2015) tested the mimetic resemblance of several sexually monomorphic and female-limited Batesian mimics, including *P. polytes*, using bird vision models. Their results show that females are better mimics than males of sexually monomorphic taxa, and that female-limited mimics are as good as sexually monomorphic mimics, supporting the idea that females disproportionately benefit from mimicry. If the benefit to mimicry derives in part from behavioral differences between the sexes, our Phase I results may reflect baseline predation that *P. polytes* experience due to visual

detection alone and in the absence of any behavior, including flight behavior and smaller movement such as body/leg/antennnal movement as well as absence of body odor.

The continuum between Batesian and Mullerian mimicry is determined by the relative unpalatability of the taxa involved (Huheey, 1975). In Batesian systems, where the mimic is palatable, both the abundance and unpalatability of the model are expected to strongly influence the mimic's benefit (Lindström et al., 1997, Finkbeiner et al., 2018). *Pachliopta aristolochiae* are known to occur at some of the experimental sites, and their relative abundances in comparison to *P. polytes* across those sites are variable (Jain et al., 2017). The degree of unpalatability of *P. aristolochiae* to bird predators is not well known and could influence how strongly birds avoid its phenotype (Speed, 2000). Feeding experiments using captive bulbuls (*Hypsipetes amaurotis*) found that birds experienced a negative physical reaction immediately after ingesting *P. aristolochiae*, and subsequently decreased their feeding on mimetic *P. polytes* (Uesugi, 1996). Interestingly, however, birds in Uesugi's experiment also showed a small decrease in feeding on non-mimetic *P. polytes* over the course of the feeding trials. This could reflect a generalization of avoidance beyond the mimicry phenotype to, for example, butterflies with black wings (Johki, 1983; Johki et al., 1986; Speed, 2000). It could also imply that *P. polytes* itself may be somewhat unpalatable. Smetacek (2006) presented freshly caught *P. polytes* to free-ranging predators in Uttaranchal, India and observed that only 44.4% were eaten by birds in comparison to 77-100% of palatable control species eaten. If reclassified, this would not be the first case in which a Batesian mimic was actually found to be an unpalatable Mullerian co-mimic (Ritland and Brower, 1991).

Predator psychology is complex and acts as the selective agent in Batesian mimicry systems (Speed, 2000). Over 100 years ago Fryer (1913) recorded detailed observations of birds

chasing and eating various butterfly species, including mimetic and non-mimetic *P. polytes* and distantly related species thought to be noxious to birds. Although we cannot deny the striking resemblance between distantly related species, the notion of mimicry is oversimplified in comparison to the dynamics taking place in nature. Artificial prey experiments have become powerful tools for mimicry research in natural settings by allowing us to manipulate the signals that predators encounter and measure predators' responses in the field. Significant advances using this method (especially for butterflies) include assessing the influence of roosting behavior on warning signals (Finkbeiner et al., 2012), studying the relative contributions of wing color versus pattern to predator deterrence (Finkbeiner et al., 2014), uncovering how eyespot size and number influence predation (Stevens et al., 2008; Ho et al., 2016), analyzing the evolution of novel colors in warning signals (Dell'Aglio et al., 2016; Finkbeiner et al., 2017b; Wee and Monteiro, 2017), and dissecting the importance of white bands (false boundaries) and disruptive coloration for protection from predators (Seymoure and Aiello 2015). Further experiments are needed that integrate phenotypic and behavioral qualities of Batesian mimics with predator psychology, and that assess the importance of model frequency dependence in Batesian systems. *Papilio* swallowtails are likely to be a key system for these studies, owing to the frequent occurrence of mimicry in this group. With these further studies the growing literature concerning the genetics of mimicry will also benefit from a better understanding of how natural selection on mimicry proceeds in natural populations.

3 The shared genetic basis of mimicry in swallowtail butterflies: common ancestry or independent evolution?

3.1 Abstract

The extent to which convergent adaptations share a genetic basis is consequential for understanding the evolutionary origins of phenotypic diversity. To address this question, we ask whether the same genes underlie polymorphic mimicry in multiple *Papilio* swallowtail butterflies. By comparing signatures of genetic variation between polymorphic and monomorphic species, we explore how ancestral variation, hybridization, or independent evolutionary trajectories contributed to wing pattern diversity in this group. We find that a single gene, *doublesex (dsx)*, controls mimicry across multiple taxa, but with species-specific patterns of genetic differentiation and linkage disequilibrium. In contrast to widespread examples of phenotypic evolution driven by introgression, our analyses indicate that *dsx* mimicry alleles are largely independently derived between species. We propose that an ancestral polymorphism drove evolutionary turnover of *dsx* alleles resulting in the wing pattern diversity of extant polymorphic and monomorphic lineages. Whether the current diversity of wing pattern mimicry in this group arose from independent co-option of *dsx* or from an ancestral polymorphism, our findings reveal a dynamic evolutionary history of *dsx*-mediated mimicry among *Papilio* butterflies.

3.2 Introduction

A diverse array of convergent adaptations are found across animal and plant taxa, arising from the interplay of natural selection, constraint, and historical contingency (McGhee, 2011).

Comparing the genetic basis of convergent traits has been central to uncovering the genomic patterns and evolutionary processes that drive adaptation and phenotypic diversification (Martin and Orgogozo, 2013). By leveraging natural experiments of convergent evolution, we are able to assess the extent to which parallel evolution proceeds with shared genetic architecture, genes, and/or mutations (Rosenblum et al., 2014). Furthermore, comparing how these evolutionary changes unfold in the genome among multiple taxa can uncover how ancestral variation, hybridization, or independent evolutionary trajectories contribute to adaptive phenotypes (Stern, 2013).

Mimicry is a major convergent adaptation that has evolved repeatedly across animals and plants (Wickler, 1968), acting as a significant driver of phenotypic evolution. Much of our knowledge about the molecular foundations and evolution of mimicry has stemmed from research on wing pattern mimicry in butterflies (Clarke and Sheppard, 1960, 1962; Clarke and Sheppard, 1972; Clarke et al., 1968; Consortium, 2012; Joron et al., 2006; Kunte et al., 2014), a fundamental adaptation known to involve a diverse set of genes and genetic architectures. Perhaps the most extreme version of this adaptation is found in polymorphic mimicry systems, where discrete mimetic phenotypes co-occur within a species. Polymorphic mimicry has evolved in multiple butterfly lineages (Joron et al., 2006; Kunte, 2009; Zakharov et al., 2004), providing an opportunity to investigate the genetic controls and evolutionary origins of this complex adaptation. In *Heliconius numata*, polymorphic mimicry is controlled by a tightly linked cluster of wing patterning genes (Joron et al., 2006), and mimicry alleles are frequently shared between *Heliconius* species through hybridization (Heliconius Genome Consortium, 2012). In the genus *Papilio*, where polymorphic mimicry is typically limited to females, several independent molecular origins have been implicated in its evolution. Classic genetic crossing experiments on

various *Papilio* species showed that either sex-linked or autosomal loci can function as 'switches' between female morphs (Clarke and Sheppard, 1960, 1962; Clarke and Sheppard, 1972), and more recent molecular work has identified and characterized some of these mimicry loci (Koch and Behnecke, 2000; Kunte et al., 2014; Nishikawa et al., 2015; Scriber et al., 1996). In each of these studies, the mimicry loci of different *Papilio* species map to distinct regions of the genome with seemingly independent functional bases. These single-species analyses have illustrated the diverse molecular underpinnings generating polymorphic wing patterns. However, a comparative analysis of multiple polymorphic and monomorphic lineages is needed to elucidate the relative contributions of factors like historical contingency and contemporary allele sharing to the evolutionary origins and trajectories of mimicry and wing pattern diversity in this group.

Polymorphic mimicry is inferred to have evolved independently along several branches of the *Papilio* tree (Kunte, 2009; Zakharov et al., 2004), but questions remain about the potential roles of ancestral variation and contemporary mimicry allele sharing in shaping the extant diversity of *Papilio* wing pattern phenotypes. Multiple *Papilio* species are known to share mimicry supergene architecture (Clarke and Sheppard, 1960; Clarke and Sheppard, 1972; Clarke et al., 1968), in which wing pattern variation is transmitted as a single Mendelian locus. More recently, studies in both *P. polytes* and *P. memnon* characterized their mimicry loci as having the same identity, the autosomal gene *doublesex* (*dsx*) (Komata et al., 2016; Kunte et al., 2014; Nishikawa et al., 2015). The *dsx* mimicry alleles are distinct between *P. polytes* and *P. memnon* (Komata et al., 2016), but without knowledge of *dsx* variation among neighboring species it is uncertain whether *dsx*-mediated mimicry arose *de novo* or is a product of shared ancestral variation. A *de novo* scenario would imply possible genetic potentiation or constraint leading to

repeated recruitment of the *dsx* locus in mimicry evolution. Conversely, the sorting of ancestral variation would mean multiple losses of mimicry, shifting the view of mimicry as an evolutionary dead-end. The extent to which *dsx* mediates polymorphic mimicry in other *Papilio* lineages and how variation at *dsx* is related between polymorphic and monomorphic lineages are thus open questions that are pivotal to understanding the roles of genetic potentiation or bias, constraint, and shared ancestry in mimicry evolution.

In this study, we test for convergence in the genetic basis of mimicry among four closely related female polymorphic lineages, *P. polytes*, *P. memnon*, *P. rumanzovia*, and *P. aegeus*. We ask whether the evolution of polymorphic mimicry among these four taxa involves changes at the same genomic location, and if so, whether the functional molecular aspects of such variation are shared between species. We also analyze the genomic signatures of their closely allied monomorphic lineages to infer the historical processes driving mimicry evolution and wing pattern diversity across this group of taxa. Our results indicate that a shared region, the gene *dsx*, controls female polymorphic mimicry among the four polymorphic species. However, we observe different patterns of association and divergence at the *dsx* locus in each lineage, indicating the presence of distinct *dsx* mimicry alleles among species. We synthesize our findings and previous work to propose that the current diversity of mimicry polymorphism and wing pattern phenotypes in this group arose from an ongoing process of evolutionary turnover at *dsx* from a polymorphic ancestor. The implications of these findings suggest a dynamic trajectory for mimicry evolution, involving many gains and losses of mimetic wing patterns.

3.3 Results

3.3.1 Identifying mimicry loci in *P. rumanzovia*, *P. memnon*, *P. aegeus*

We first identified the mimicry loci of *P. rumanzovia*, *P. memnon*, and *P. aegeus* using genome-wide association studies (GWAS) and principal component analyses (PCA) of single nucleotide polymorphism (SNP) data. We analyzed female specimens representing three *P. rumanzovia* morphs (simple, blended, white), two *P. memnon* morphs (band, patch), and two *P. aegeus* morphs (light, dark).

In *P. rumanzovia*, a GWAS with the three morphs and 869,047 SNP variants revealed a single peak of association positioned within the *dsx* gene (Figure 8A). In additional GWAS comparing pairs of morphs we observed the same peak of SNPs in the *dsx* region for the simple/white and blended/white comparisons, but not for the simple/blended (Figure 9). For the simple/blended GWAS, only one highly associated SNP remained within the *dsx* region, but several emerged in the vicinity of *dsx* (Figure 9C). A PCA of approximately 2.5 million genome-wide SNPs showed one population cluster that included most of the individuals (Figure 8B). A PCA based on 779 SNPs from the *dsx* region, however, resulted in the white individuals separating from dark and blended individuals along PC1 (Figure 8C). All but one of the white individuals were heterozygous at *dsx*, and thus were localized at the center of PC1 (Figure 8C). These results suggest that variation at the *dsx* locus differentiates the *P. rumanzovia* white patch morph from the dark and blended morphs, and that the dark and blended morphs may be determined by variation in and around *dsx*.

The GWAS for *P. memnon* using approximately 1.8 million variants showed more noise in genome-wide association values, but the densest cluster of highly associated SNPs fell within

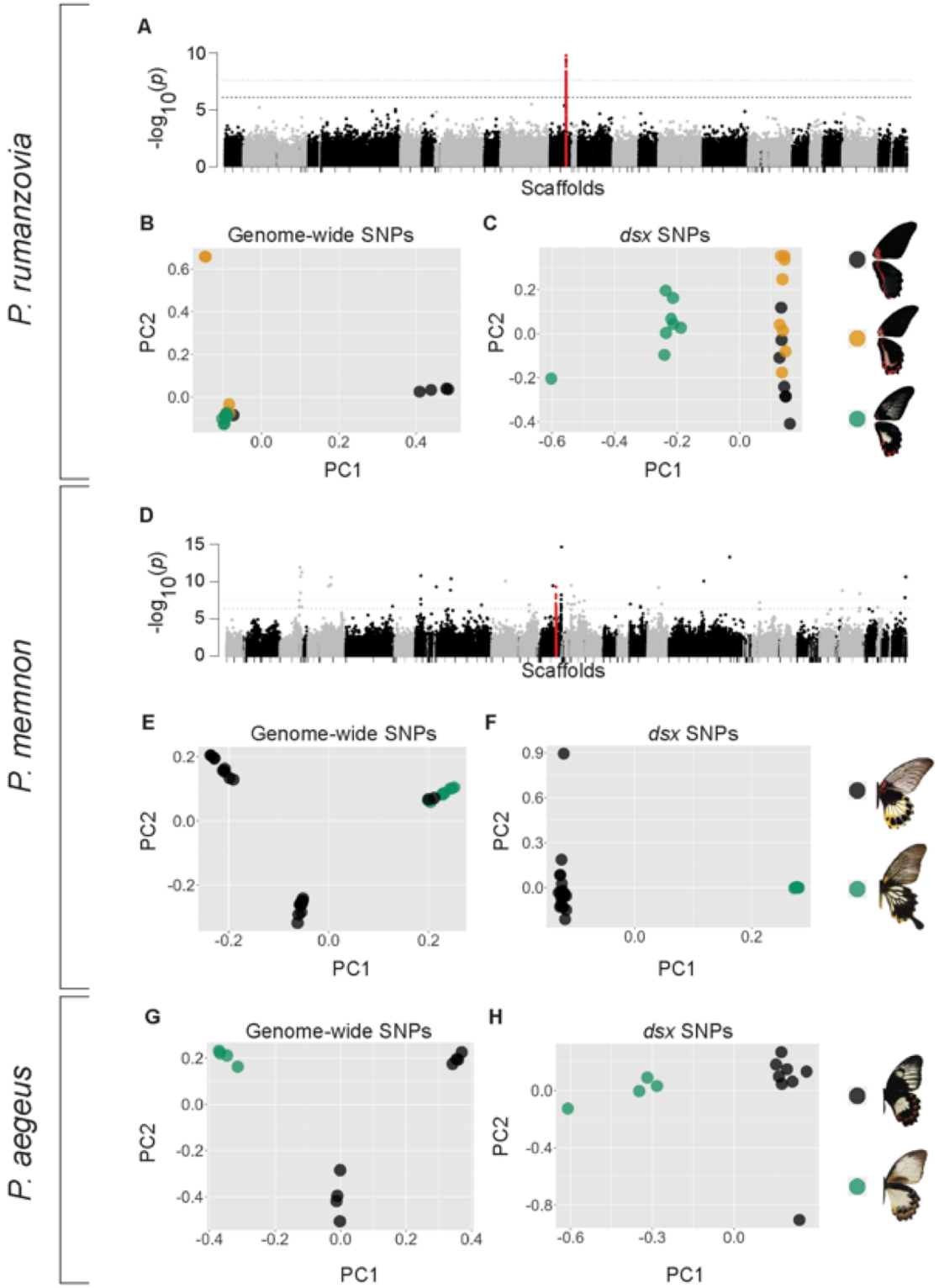

Figure 8 | Genome-wide association studies and principal component analyses identifying mimicry loci in *P. rumanzovia*, *P. memnon*, and *P. aegeus*. Red points in A and D indicate SNPs in the *dsx* region. Dashed and dotted lines show the false discovery rate (q value) cutoffs of 0.01 and 0.001, respectively.

the *dsx* region (Figure 8D). The PCA with genome-wide SNPs (approximately 2.5 million SNPs) revealed 3 population clusters (Figure 8E). Two population clusters were homogeneous for wing pattern, and one population cluster contained individuals of both wing pattern morphs, suggesting a confounding signal of population structure in the GWAS. PCA based on 644 *dsx* SNPs using the full set of individuals and using only the population cluster containing two morphs produced the same pattern of individuals segregating by phenotype along PC1 (Figure 8F). These results point to *dsx* as the mimicry locus in *P. memnon*, consistent with the recent finding of two *dsx* allelic sequences corresponding to different female wing patterns (Komata et al., 2016).

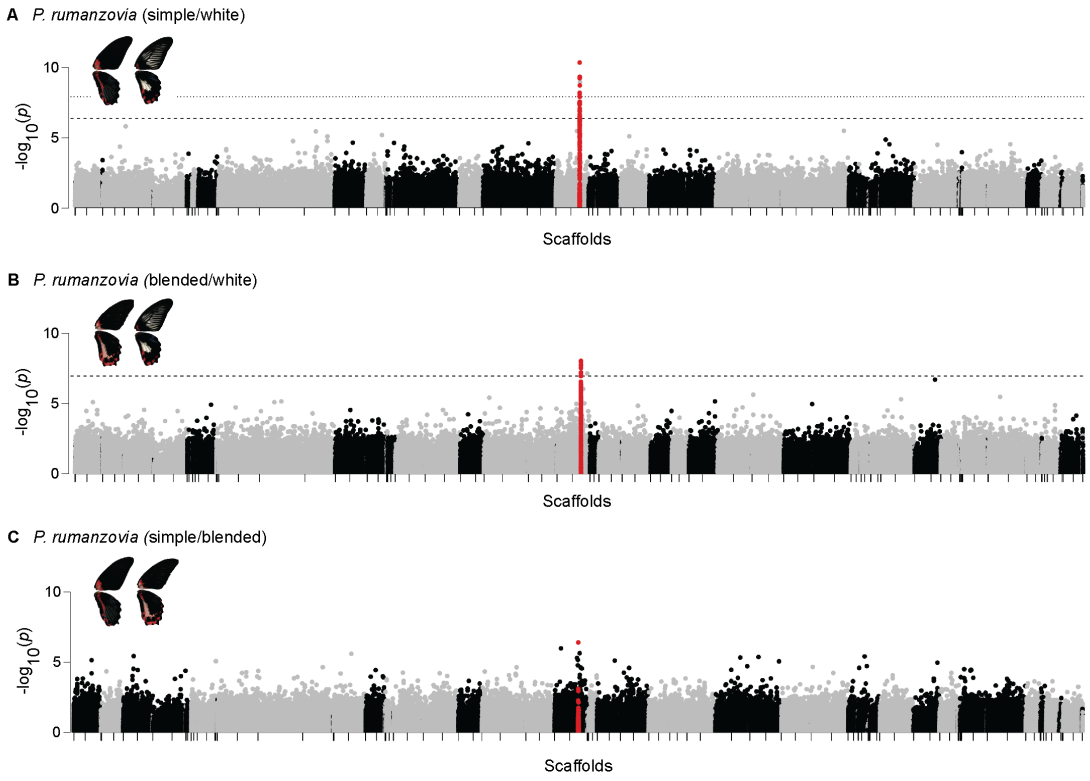

Figure 9 | Pairwise genome-wide association studies for *P. rumanzovia*. Red points indicate SNPs in the *dsx* region. Dashed and dotted lines show the false discovery rate (q value) cutoffs of 0.01 and 0.001, respectively. The q value lines could not be drawn for C because the lowest q value observed was 0.31.

We were not able to generate GWAS results for *P. aegeus* due to low sample size. The PCA for approximately 1.5 million genome-wide SNPs revealed three population clusters (Figure 8G), but the PCA with only *dsx* SNPs (500 SNPs) showed individuals segregating by phenotype along PC1 (Figure 8H). Like in *P. rumanzovia*, the light individuals were nearly all *dsx* heterozygotes and fell in the center of PC1 (Figure 8H). From these results, we concluded that *dsx* is also associated with polymorphic wing patterning in *P. aegeus*.

3.3.2 Signatures of genetic divergence and linkage across *dsx* in *P. rumanzovia*, *P. memnon*, and *P. aegeus*

We calculated F_{ST} between wing pattern morphs within each polymorphic species to analyze patterns of divergence at the mimicry locus *dsx*. For each comparison, we applied a 10kb window size across the genome and removed windows with a low number of variants (bottom 10% by species). First, we calculated F_{ST} between the mimetic and non-mimetic *P. polytes* female morphs as a positive control for highly divergent, inverted *dsx* haplotypes (Kunte et al., 2014; Nishikawa et al., 2015). We observed a plateau of elevated F_{ST} across the entire *dsx* region, reflecting the known inverted chromosomal structure of *dsx* in *P. polytes* (Figure 10A). Furthermore, the peak F_{ST} value for *dsx* windows was an extreme outlier compared to the genome-wide distribution of F_{ST} values (Figure 10). In subsequent comparisons for *P. rumanzovia*, *P. memnon*, and *P. aegeus*, each species showed elevated F_{ST} at *dsx* relative to the rest of the genome, but we observed species-specific patterns of divergence within the *dsx* region. For *P. rumanzovia* we excluded the individuals outside of the main population cluster based on the genome-wide PCA (Figure 8B) to avoid the effects of population structure, and also excluded the heterozygous *dsx* individuals based on the *dsx* PCA (Figure 8C) to obtain the most

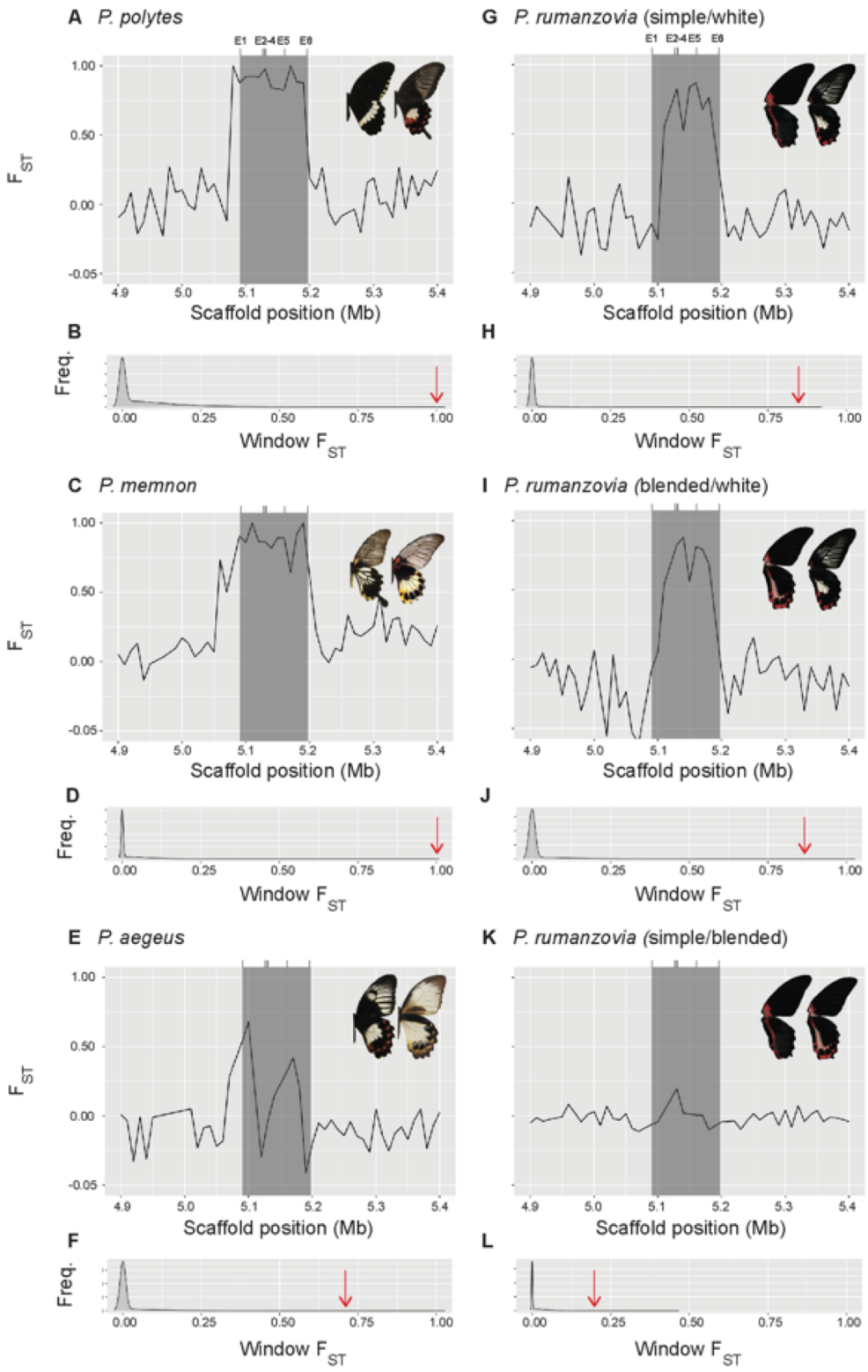

Figure 10 | F_{ST} across a 500kb interval containing *dsx* (grey box) and genome-wide F_{ST} distributions. E1-6 indicate the *dsx* exons. Red arrows indicate the peak value for *dsx* windows.

polarized divergence signatures for the region of interest. The results showed high F_{ST} for *dsx* windows in comparisons between simple/white and blended/white, consistent with the GWAS and PCA results, but this signature was present only from the vicinity of exon two to exon six (Figure 10G, I). The peak F_{ST} values for *dsx* windows between simple/white and blended/white were also extreme outliers to genome-wide F_{ST} values (Figure 10H, J). Between the simple and blended morphs, only one *dsx* window was moderately elevated, driven by the single highly associated SNP we observed in the GWAS (Figure 10K, Figure 9C). For *P. memnon* we included only the individuals belonging to the polymorphic population cluster based on the genome-wide PCA (Figure 8E) given the clear population structure among the samples. The entire length of *dsx* showed elevated F_{ST} in *P. memnon*, resembling the F_{ST} signature observed for *dsx* in *P. polytes* (Figure 10C). For *P. aegeus* we were not able to exclude individuals based on genome-wide population clustering (Figure 8G), but we did exclude *dsx* heterozygotes using the *dsx* PCA results (Figure 8H). The elevated *dsx* F_{ST} signature in *P. aegeus* was concentrated in a single window containing exon one (Figure 10E). The peak F_{ST} values for *dsx* in both *P. memnon* and *P. aegeus* were extreme relative to genome-wide values, consistent with earlier GWAS and PCA (Figure 10D, F).

We next analyzed patterns of linkage disequilibrium (LD) within *dsx* and the surrounding region for each species, again using the two *P. polytes* female morphs as a positive control. *P. polytes* showed high LD across the entire length of *dsx*, consistent with prior analyses and the known inversion spanning the *dsx* region (Nishikawa et al., 2015) (Figure 11A). In *P. rumanzovia*, a subset of the *dsx* region spanning exons two through six showed elevated LD, reflecting the F_{ST} signatures described above (Figure 11B, Figure 10G, I). For *P. memnon* we observed a region of elevated LD pattern across the length of *dsx* as in *P. polytes*, corroborating

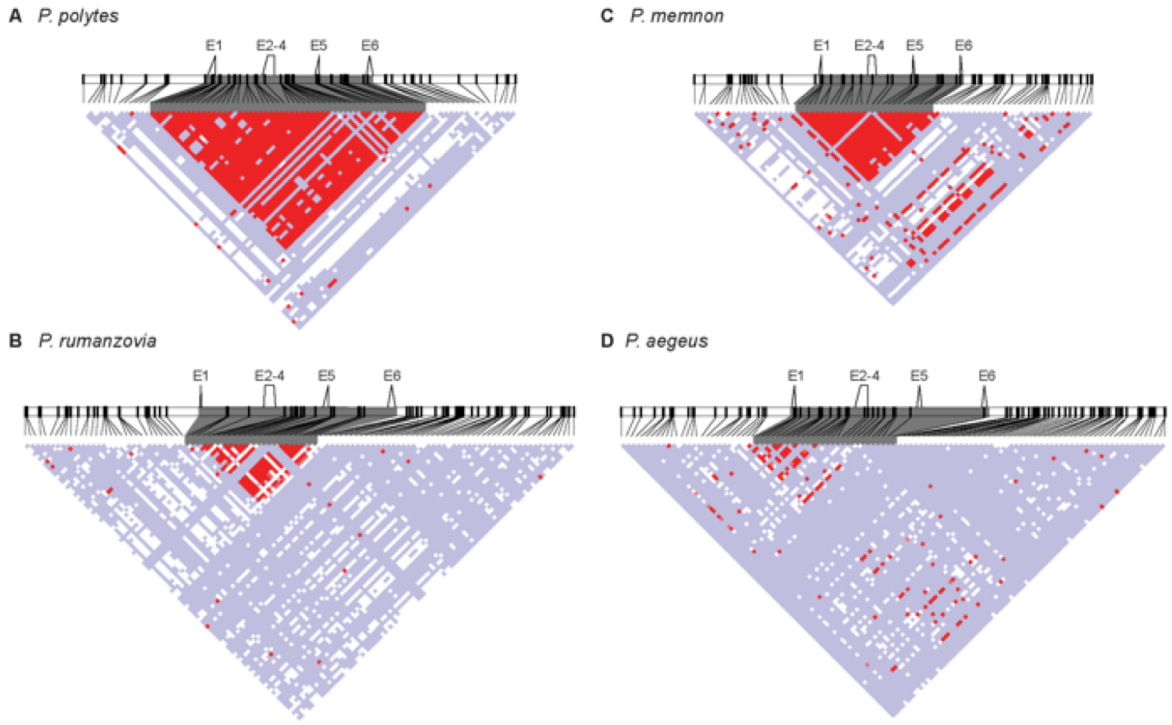

Figure 11 | Linkage disequilibrium (LD) heat map across *dsx* (grey shading) and flanking 100kb. Standard color scheme: D'<1, LOD<2 (white); D'=1, LOD<2 (blue); D'≤1, LOD≥2 (pink and red). E1-6 indicate the *dsx* exons.

the high F_{ST} plateau across this region (Figure 11C, Figure 10C). The elevated LD signature for *dsx* in *P. aegeus* was localized to a region containing exon one, which was also consistent with F_{ST} signatures (Figure 11D, Figure 10E).

3.3.3 *De novo* genome assembly in *P. rumanzovia*

We generated *de novo* genome assemblies for *P. rumanzovia* to validate our methods and explore structural variation at *dsx*. We used combined mate-pair and paired-end sequencing datasets to assemble the genomes of one female that we inferred to be homozygous for the simple morph-associated haplotype and one female inferred to be homozygous for the white morph-associated haplotype. The assembled genome sizes for the simple and white morph were

218 and 215 Mb, respectively, which are similar to the 227Mb *P. polytes* genome (Kunte et al., 2014; Nishikawa et al., 2015). The scaffold N50 values for the simple and white assemblies were 53kb and 197kb, respectively. We identified four scaffolds in the simple morph assembly and three scaffolds in the white morph assembly that contained *dsx* exons (Figure 12). In the simple morph assembly, two scaffolds provided structural information. First, exons two through four were assembled on a single scaffold, at approximately the same distance and orientation to one another as in *P. polytes*. Second, exon six and the neighboring *ubiquitously expressed transcript* (UXT) were assembled together, revealing the collinearity of the simple morph with the non-mimetic *P. polytes* morph and with the outgroup taxon *P. xuthus* (Nishikawa et al., 2015). With the white morph assembly, we could only gather structural information from one scaffold which contained exons one through four arranged at approximately the same distance and orientation as in *P. polytes*. Our comparisons of the simple and white morph showed a sharp increase in F_{ST} and LD between exons one and two, and a drop in these signatures between exons five and six (Figure 10G, 11B), which could be indicative of a chromosomal inversion in this region. This inversion would have to be in the simple morph, given the white morph scaffold contained exons one through four, and these were collinear with *P. polytes*.

We aligned the scaffolds containing *dsx* exons to further explore sequence divergence between the *P. rumanzovia* simple and white morphs (Figure 12). Consistent with the F_{ST} signatures (Figure 10G), we generally observed higher sequence identity surrounding exon one and much lower identity for regions surrounding exons two through six. In contrast to the numerous substitutions between the *P. polytes* mimetic and non-mimetic across exons one through six, we found that the simple and white *P. rumanzovia* sequences had identical sequences for exons one through four and differed only at exons five and six. In *P. polytes* exon

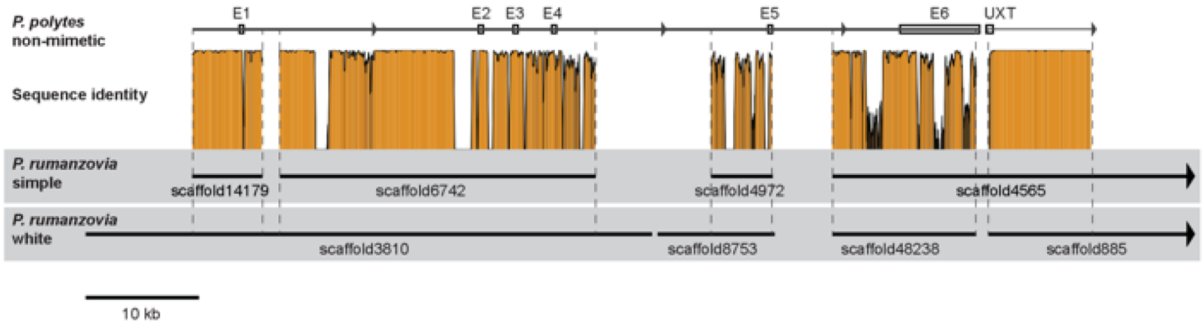

Figure 12 | Schematic of the *P. polytes dsx* region and scaffolds containing *dsx* exons from *P. rumanzovia* simple and white morph *de novo* genome assemblies. Sequence identity is shown between homologous *P. rumanzovia* scaffolds based on sliding 100bp windows. E1-6 denote *dsx* exons and UXT denotes the coding sequence of the neighboring *ubiquitously expressed transcript*. The physical orientation is flipped to match the orientation shown in earlier figures.

five is only spliced into the male *dsx* isoform, and exon six is a non-coding exon (Kunte et al., 2014). While we cannot conclude what the functional impacts of these differences are, these results appear to indicate that the switching between female mimicry phenotypes in *P. rumanzovia* is not a result of *dsx* protein coding differences, but likely a regulatory phenomenon.

Surprisingly, our findings for *P. rumanzovia*, *P. memnon*, and *P. aegeus*, along with previous work on *P. polytes* (Kunte et al., 2014; Nishikawa et al., 2015; Zhang et al., 2017) and *P. memnon* (Komata et al., 2016), indicate a shared genetic basis for female-limited polymorphic mimicry. However, contrasting patterns of genetic differentiation and linkage disequilibrium across the *dsx* region among species may reflect different molecular mechanisms underlying *dsx*-mediated mimicry. We next sought to explore the evolutionary history of *dsx*-mediated polymorphic mimicry in *Papilio*, and whether this common basis for polymorphic mimicry resulted from allele sharing of the same *dsx* haplotypes.

3.3.4 Evolutionary relationships between *dsx* haplotypes

In order to trace the evolutionary history of *dsx*-mediated wing pattern polymorphism we characterized the phylogenetic relationships of polymorphic and monomorphic *Papilio* species using both genome-wide SNPs and phased *dsx* SNPs. We generated a maximum-likelihood species tree based on approximately 3.4 million SNPs from the coding sequence of 51 individuals representing 16 monomorphic and 4 polymorphic species (Figure 13A; Table S1). Our topology was largely consistent with published phylogenies (Condamine et al., 2012; Zakharov et al., 2004; Zhang et al., 2017), but included taxa that had not been sampled in previous phylogenies. We then phased approximately 7000 SNPs from the *dsx* region and built a maximum-likelihood gene tree for 116 individuals (Table S1). The *dsx* gene tree topology mirrored the species tree topology, with the polymorphic haplotypes clustering by species (Figure 13B). We observed no clustering of haplotypes between species indicative of *dsx* allele sharing.

We were surprised to find all mimicry haplotypes clustering by species in the *dsx* gene tree, with no apparent allele clustering between species. However, recombination or gene conversion between *dsx* haplotypes within species could erode signatures of allele sharing due to ancestry or hybridization. Gene conversion occurs when one allelic sequence is copied onto its homolog during DNA repair, resulting in homogenization of alleles over lengths of 100-2000bp (Korunes and Noor, 2017). We tested for gene conversion between *dsx* haplotypes within each polymorphic species using GENECONV (Sawyer, 1999) and found two significant tracts of identical sequence (Table 5). The first was in *P. polytes*, and coincided with a region of decreased F_{ST} (Table 5; Figure 10A). The second putative gene conversion tract was between the *P. rumanzovia* simple and white morphs, and also coincided with the low F_{ST} and LD signatures

observed for that part of the *dsx* region (Table 5; Figure 10G, Figure 11B). However, given the extended lengths of these putative tracts compared to typical gene conversion events, these regions appear to reflect areas of double cross-over events within *dsx* alleles.

To further investigate the possibility of *dsx* allele sharing, we generated maximum-likelihood *dsx* trees based on regions of maximum divergence between morphs. If *dsx* alleles are shared between species, gene conversion or recombination within species would erode these signatures while areas of high allelic divergence might retain them. We extracted two regions from the approximately 7000 phased *dsx* SNP alignment corresponding to the high F_{ST} windows within *P. rumanzovia* (simple/white and blended/white; approximately 3800 SNPs, 5.13-5.19 Mb) and *P. aegeus* (625 SNPs, 5.09-5.1 Mb), and constructed a maximum-likelihood tree for each region (Figure 13C, D). The first tree topology was slightly different in its placement of some monomorphic taxa, but showed the same pattern of *dsx* haplotypes clustering by species for the polymorphic taxa (Figure 13C). The second tree topology maintained the clustering by species of the *P. aegeus* and *P. polytes* haplotypes, but shifted the grouping of *P. rumanzovia* and *P. memnon* sequences (Figure 13D). We observed the *P. rumanzovia* white morph nested within the *P. rumanzovia* simple and blended morphs, consistent with the low F_{ST} for this region (Figure 10G, I), and these sequences were grouped with the *P. memnon* band morph. This result could indicate that both *P. rumanzovia* and *P. memnon* inherited ancestrally polymorphic *dsx* alleles, a subset of which we observed in this analysis. Alternatively, *P. rumanzovia* could have originated exclusively from the *P. memnon* band morph, inheriting a single *dsx* haplotype but subsequently evolving polymorphism via new *dsx* alleles. Under either of these scenarios, the monomorphic taxa in the *P. memnon*/*P. rumanzovia* subgroup would have each fixed a single *dsx* haplotype (Figure 10A, D). With the exception of the clustering between *P. rumanzovia* and the *P. memnon*

band morph, our results show no evidence of common ancestry between polymorphic taxa of individual *dsx* haplotypes.

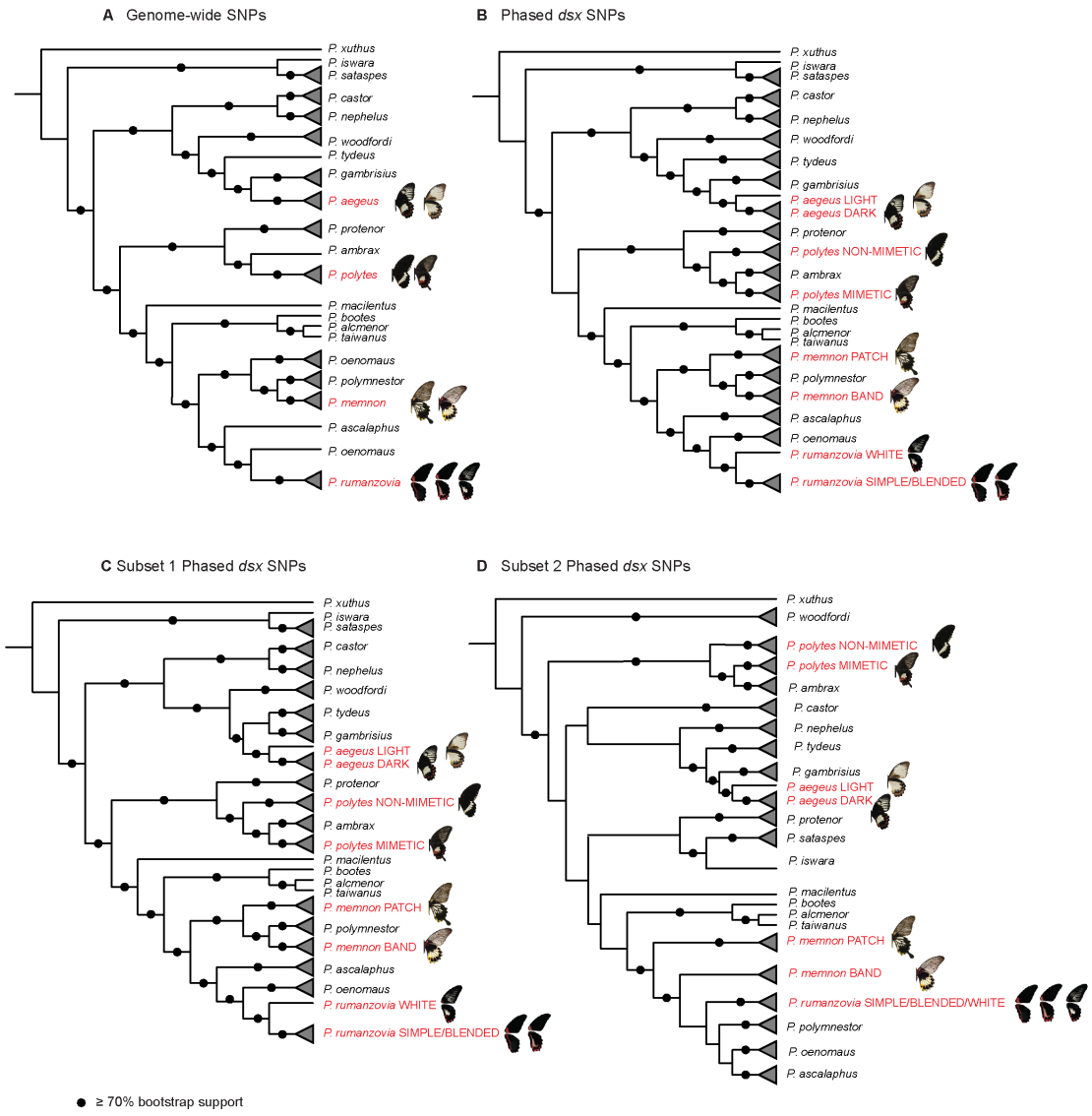

Figure 13 | Maximum-likelihood phylogenies for polymorphic (red) and monomorphic (black) *Papilio* butterflies based on genome-wide SNPs (A) and phased *dsx* SNPs (B). Trees C and D are maximum-likelihood trees based on phased SNPs for subsets of the *dsx* region (5.13-5.19 Mb and 5.09-5.1 Mb, respectively).

Table 5 | Putative gene conversion tracts between *dsx* haplotypes.

Species	Morphs	Sim P value[a]	BC KA P value[b]	Start (bp)	End (bp)	Length
P. polytes	Mimetic/ non-mimetic	0.0029	0.12122	5148362	5160925	12564
P. rumanzovia	Simple/white	0.0167	0.50317	5090846	5118037	27192

[a] Sim P value based on 10,000 permutations

[b] Bonferroni-corrected Karlin-Altschul P value

3.4 Discussion

Our study reveals a dynamic history of mimicry and wing pattern evolution within *Papilio* involving changes at a single autosomal gene, *dsx*. This same gene controls polymorphic mimicry in multiple *Papilio* species. By leveraging a comprehensive genomic dataset of polymorphic and monomorphic lineages, we are able to infer the evolutionary processes that have shaped mimicry and wing patterning in this group. We find evidence consistent with either independent co-option of *dsx* or sorting of ancestral polymorphism, and reject introgression as a mechanism for mimicry evolution in this group.

dsx is known for its fundamental role in somatic sex differentiation across insects, and has been implicated in sexually dimorphic adaptations essential to reproduction such as the sex combs and courtship neurons of *Drosophila*, and horns in *Onthophagus* beetles (Kijimoto et al., 2012; Kimura et al., 2008; Tanaka et al., 2011). The role of *dsx* in polymorphic mimicry, however, presents a departure from other *dsx*-mediated traits in that multiple, distinct forms are

maintained among females, and the evolution of these forms is tied to predator avoidance rather than courtship or reproduction. Female-limited polymorphic mimicry in *P. polytes* encompasses variation not only in wing pattern and shape, but also in flight-related traits like minimum wing positional angle, wingbeat frequency, and flight trajectory (Kitamura and Imafuku, 2010, 2015). in *P. polytes dsx* is known to undergo alternative splicing (Burtis and Baker, 1989) and tissue-specific expression (Kunte et al., 2014; Williams and Carroll, 2009) to control the development of sex-specific features, possibly facilitating the evolution of these additional mimicry-related traits. How *dsx* acquired mimicry-related functions integrating color, shape, and flight behavior remains an important question warranting further investigation.

Although we find the same gene underlying polymorphic mimicry across taxa, our comparisons reveal species-specific patterns of genetic variation and linkage disequilibrium in the *dsx* region. In *P. polytes* the mimetic and non-mimetic *dsx* haplotypes differ by thousands of substitutions in their coding and non-coding sequence, and an inversion spans the entire *dsx* gene, possibly affecting neighboring gene function (Kunte et al., 2014; Nishikawa et al., 2015; Zhang et al., 2017). In contrast *P. rumanzovia* showed an extended region of divergence across exons two through six of *dsx*, but only distinguishing the white morph from the simple and blended morphs. We found that these differences in *dsx* sequence were almost exclusively in the non-coding regions of the gene. Together, these patterns indicate a regulatory functional mechanism for *dsx*-mediated polymorphic mimicry in *P. rumanzovia*, which is consistent with the idea that variation in the coding sequence of the mimetic *P. polytes* allele does not influence mimicry (Zhang et al., 2017). In *P. memnon* we saw signatures more similar to *P. polytes*, including sequence divergence across the entirety of *dsx* and substitutions in both coding and non-coding sequence. For *P. aegeus*, however, we observed differentiation between morphs in

coding and non-coding sequence mostly around exon one, which comprises approximately 60% of the Dsx protein. While we cannot pinpoint the precise mutations that drive female development into alternative morphs, these results suggest different contributions of *dsx* non-coding and coding variation, and consequently different molecular mechanisms, acting between *Papilio* species. The extreme F_{ST} and LD signatures at *dsx* observed across the polymorphic species could reflect the presence of species-specific chromosomal inversions associated with maintaining polymorphic alleles. Our limited structural information from *P. rumanzovia*, however, does not reveal conclusive evidence for an inversion polymorphism in the *dsx* region.

Mimicry has been regarded as an evolutionary dead-end, where species either retain mimicry or go extinct, but do not lose it (Kunte, 2009; Savage and Mullen, 2009; Zakharov et al., 2004). Past work based on ancestral state reconstruction inferred that female-limited polymorphic mimicry arose independently in *P. polytes*, *P. aegeus*, and in the ancestor of *P. rumanzovia* and *P. memnon*, finding no evidence for mimicry loss (Kunte, 2009). Our findings, however, suggest a more complex and dynamic evolutionary history that may involve multiple gains and losses of mimicry. With genomic-level coverage and expanded taxonomic sampling, our dataset builds a more comprehensive view of wing pattern evolution. If our results had revealed different mimicry genes among the polymorphic species, this would have supported previous studies proposing mimicry as a dead-end. While our finding of a shared mimicry gene could still be consistent with a scenario of independent evolution, this may also reflect other evolutionary processes involving the sorting of ancestral variation or recent allele sharing. With the possibility that these other processes contribute to wing pattern evolution, we cannot definitively rule out the repeated loss of mimicry.

Shared *dsx*-mediated mimicry could result from different evolutionary scenarios including independent co-option, introgressive hybridization, and sorting of ancestral polymorphism. With independent evolutionary co-option of *dsx*, we would expect to find species-specific *dsx* haplotypes, which is consistent with our observation of independent *dsx* haplotypes between species. In contrast, a scenario of introgressive hybridization would spread shared *dsx* haplotypes between multiple species. We find no evidence to support introgression of mimicry alleles between species in this study. The third scenario of sorting ancestrally polymorphic *dsx* alleles could produce various signatures, some of which are consistent with our results. In the simplest case, a polymorphic ancestor would pass multiple *dsx* alleles to each of its polymorphic descendant lineages, resulting in a pattern of *dsx* allele sharing across these lineages. We clearly do not observe this type allele sharing. Alternatively, descendant lineages could each retain different alleles, causing the surviving alleles to appear independent between lineages. In a more complex version of this process, individual lineages could independently lose a subset of *dsx* alleles, generate new alleles, or fix a particular allele. This process of allelic turnover would produce a variety of polymorphic taxa with seemingly distinct ancestry at *dsx*, and would result in many losses of mimicry.

We contend that an ongoing process of allelic turnover at *dsx* from a polymorphic ancestor likely gave rise to the distinct mimicry haplotypes observed between polymorphic species and the diversity of monomorphic haplotypes in their closely-related allies. While we cannot rule out independent co-option, examples from this group support the allelic turnover process. For instance, a recent study found that an additional mimetic haplotype independently arose in each of two *P. polytes* subspecies in the course of approximately 1.7 MY (Zhang et al., 2017). This illustrates the rapid timescales at which novel mimicry alleles can arise from

polymorphic ancestors. In another example from the same study, Zhang *et al.* (Zhang et al., 2017) found that *P. phestus* and *P. ambrax* evolved from a polymorphic ancestor but secondarily lost polymorphism, retaining only the mimetic *dsx* allele. Our results with *P. rumanzovia* and *P. memnon* show perhaps a similar example, but with a different evolutionary outcome. We observed that all *P. rumanzovia dsx* haplotypes had partially shared sequence with the *P. memnon* band morph, implying that *P. rumanzovia* might have originated as a monomorphic mimic and subsequently gained polymorphism. Together these examples show a dynamic evolutionary landscape for *dsx* alleles driving shifts in the wing pattern diversity of this group.

Descendance from a polymorphic ancestor would imply multiple cases of mimicry loss in the lineages surrounding polymorphic taxa. This would contrast with earlier work in butterflies (Komata et al., 2016; Savage and Mullen, 2009) and contribute to the shifting views on mimicry evolution, spurred by a recent study on coral snake mimicry (Rabosky et al., 2016). By integrating comprehensive comparative datasets, Davis Rabosky et al. found widespread losses of mimicry over an extensive phylogenetic scale (Rabosky et al., 2016). Their findings explicitly rejected the evolutionary irreversibility of mimicry in snakes, and may reflect broad-scale patterns across vertebrate and invertebrate groups coming to light through further integrative analyses. Continued sampling spanning the full diversity of wing pattern phenotypes in our study clade will be central to unraveling questions of relatedness between *dsx* haplotypes and the evolutionary trajectory of mimicry.

3.5 Methods

3.5.1 Sample preparation and sequencing

130 adult butterflies were collected from the wild and from butterfly farms (Table S1). Approximately 10mg of thoracic tissue was removed from each individual and genomic DNA was extracted using a chloroform-based protocol. 100bp paired-end libraries were prepared using the KAPA Hyper Prep Kit. *P. rumanzovia* libraries were sequenced on an Illumina HiSeq2500 and all others were sequenced on an Illumina HiSeq4000. Raw reads were demultiplexed based on their barcodes (Table S1).

3.5.2 Data collection and genotype calling

We chose to use the monomorphic outgroup species *P. xuthus* as the reference genome for all read-mapping instead of the more closely related *P. polytes* to avoid biasing our results with a polymorphic reference. We downloaded the *P. xuthus* v1.0 genome from PapilioBase (Nishikawa et al., 2015) and *P. polytes* resequencing data from three homozygous mimetic and three homozygous non-mimetic females from NCBI (SRR1118152, SRR1118150, SRR1118145, SRR1112619, SRR1112070, SRR1111718) (Kunte et al., 2014). Reads from the 136 total genome resequencing datasets were quality trimmed using SLIDINGWINDOW:4:15 in Trimmomatic (Bolger et al., 2014) and remaining reads were mapped to the *P. xuthus* v1.0 genome using the --very-sensitive-local option in Bowtie2 (Langmead and Salzberg, 2012). Mapped reads were then re-ordered, sorted, and deduplicated with Picard (http://picard.sourceforge.net). We called variants using GATK's (McKenna et al., 2010) HaplotypeCaller with options --emitRefConfidence GVCF --heterozygosity 0.01 -

stand_call_conf 50.0 and performed joint genotyping using GenotypeGVCFs. For SNPs we filtered out the bottom 10% by quality and with FS > 60.0 and ReadPosRankSum < -8.0, and for indels we filtered out the bottom 10% by quality and with FS > 200.0 and ReadPosRankSum < -20.0 using GATK's VariantFiltration.

3.5.3 Genome-wide association testing (GWAS) and principal component analyses (PCA)

VCF files containing SNP and indel calls were converted to PLINK format using VCFTools (Danecek et al., 2011). Phenotypes were assigned using a custom script and files were converted to GEMMA input using PLINK (Purcell et al., 2007). We used GEMMA (Zhou and Stephens, 2012) to perform association tests between genotypes and wing pattern phenotype using option -miss 0.20. Benjamini-Hochberg false discovery rate (q value) (Benjamini and Hochberg, 1995) cutoffs of 0.01 and 0.001 were calculated for each GWAS in R (R Core Team, 2017) and manhattan plots were generated using the qqman R package (R Core Team, 2017; Turner, 2014). We used PLINK (Purcell et al., 2007) to perform PCA using only SNP calls and option --geno 0.1. PCA plots were generated using the ggplot2 package in R (R Core Team, 2017; Wickham, 2016).

3.5.4 F_{ST} signatures

We calculated Weir and Cockerham's F_{ST} (Weir and Cockerham, 1984) in 10kb windows across the genome based on SNP calls using VCFTools (Danecek et al., 2011) with options --weir-fst-pop and --fst-window-size 10000. We calculated the distribution of the number of variants per window for each pairwise comparison and removed windows in the bottom 10%

because these windows are more likely to show artificially extreme F_{ST} values. F_{ST} line graphs and distributions were plotted with the ggplot2 R package (R Core Team, 2017; Wickham, 2016).

3.5.5 Linkage disequilibrium (LD) analysis

VCF files containing SNP calls across *dsx* and the flanking 100kb were converted to Haploview format using PLINK (Purcell et al., 2007). A random subset of biallelic variants was selected using PLINK's --thin option to yield approximately 1000 representative variants per species. We used Haploview (Barrett et al., 2004) to calculate pairwise LD between variants with a minimum genotyping rate of 75% and minimum minor allele frequency of 0.001. LD heat maps were exported from Haploview.

3.5.6 *De novo* genome assembly

We used genomic DNA extracted for paired-end sequencing to generate mate-pair libraries for two *P. rumanzovia* samples: one homozygous simple morph female and one homozygous white morph female. We size-selected DNA using the BluePippin platform (Sage Science) and constructed 3kb mate-pair libraries using the Nextera Mate Pair Library Prep Kit (Illumina). We assembled the combined dataset of 100bp paired-end and 3kb mate-pair libraries for each individual using Platanus (Kajitani et al., 2014). With each assembly, we then used BLAST (Altschul et al., 1990) and BLAT (Kent, 2002) to find scaffolds containing *dsx* exons, using the *P. polytes dsx* exons as the queries. Once we had identified the relevant scaffolds we aligned them using MAFFT (Katoh et al., 2002) and calculated sequence identity between the aligned regions with sliding 100bp windows in Geneious (Kearse et al., 2012).

3.5.7 Genome-wide and *dsx* phylogeny estimation

Approximately 3.4 million SNP calls from genome-wide coding sequence for 50 high quality individuals representing 4 polymorphic species and 16 monomorphic species were aligned in Geneious (Kearse et al., 2012) and converted to PHYLIP format. We inferred a genome-wide maximum-likelihood tree using the GTRGAMMA model with 100 bootstraps in RAxML (Stamatakis, 2014). The RAxML output was uploaded to iTOL (Letunic and Bork, 2006) to create the tree image.

We phased 6730 SNPs from the *dsx* region for 116 individuals representing 4 polymorphic species and 16 monomorphic species using BEAGLE (Browning and Browning, 2007). In order to generate the most reliable phasing results for the polymorphic species, we used only individuals homozygous for alternate *dsx* haplotypes. We aligned sequences and converted them to PHYLIP format in Geneious (Kearse et al., 2012) and constructed a maximum-likelihood trees with RAxML (Stamatakis, 2014) using the GRTGAMMA model and 100 bootstraps. We constructed the tree images by uploading the RAxML outputs to iTOL (Letunic and Bork, 2006).

3.5.8 Gene conversion analysis

We used GENECONV (Sawyer, 1999) software to test for gene conversion between *dsx* haplotypes. GENECONV searches for tracts of shared sequence bounded by variable sites between alleles. The software then assesses significance using permutation testing and corrects significance values for multiple comparisons and sequence length. We used a phased full *dsx* region alignment (~100kb) of all the *dsx* haplotypes from the polymorphic taxa as input and options -Seqtype=SILENT to minimize false positives (Ezawa et al., 2010; Ezawa et al., 2006).

Future Works

The work contained in this dissertation has uncovered a number of additional questions and new avenues of research to pursue in the future. My review of the Darwin's finch system in Chapter 1 highlighted the importance and promise of integrating genomic analyses with studies rooted in field biology and natural history. Using the genus *Papilio* of swallowtail butterflies, I then addressed the ecology and evolution of polymorphic wing pattern mimicry in Chapters 2 and 3. My findings showed a modest selective advantage for mimetic morphs in terms of predator avoidance and that sex differences in life history likely promote the evolution of sexually dimorphic mimicry. Further efforts, however, are needed to characterize selection on polymorphic mimicry over broader spatial and temporal scales, explicitly considering predator psychology. Among different *Papilio* species, I also found that the same gene controls mimetic polymorphism, but with mostly independent haplotypes between species. These results suggest that the loss of mimicry and polymorphism may be more common than previously thought, but more work is needed to understand the developmental genetic basis of polymorphic mimicry and how this relates to the contrasting signatures of *dsx* variation observed between *Papilio* lineages.

While a vast body of research focuses on mimicry, investigating how mimicry operates in nature reveals a complex reality shaped by interrelated parts. What we know about model-mimic relationships often stems from human observation. These relationships must be tested using the sensory systems of relevant predators to understand if and how frequently predators will avoid the warning phenotypes of the purported models and mimics. This interaction is at the core of fundamental theory on the maintenance of mimetic polymorphism through negative frequency-dependent selection, but efforts to quantify predator aversion in mimicry systems are few. My

predation study, and another recent study, inferring predation on wild-caught *Papilio* (Komata et al., 2017) report only a slight advantage to mimetic morphs. It is not unclear, however, if these findings can be generalized to other populations or taxa. More work is needed to track predation pressure on mimics over time, and ask whether predation fluctuates with changes in the frequencies of mimics and models. Similarly, the overlapping spatial distributions of predators, models, and mimics were theorized to play a central role in determining the efficacy of mimicry, but the effects of changing and degrading natural habitat on this adaptation are not well understood. A valuable future analysis would track population sizes of models and mimics with a long-term study, and quantify predator aversion to models to better understand what model to mimic ratios can be sustained.

Spatial and temporal studies of models and mimics also have the potential to help explain the phylogenomic signatures that we observed in Chapter 3. These analyses showed many instances of loss of polymorphism among *Papilio*, sometimes resulting in the fixation of mimetic alleles. In some cases, these events appear to result from a combination of natural selection and genetic drift acting on low population sizes, and are associated with dispersal to isolated islands that are part of a fragmented habitat (Zhang et al., 2017). By combining surveys of geographic distributions of *Papilio* taxa and their respective wing pattern morphs with historical demographic modeling based on genomic sequences, we could better understand if population bottlenecks are a significant feature driving wing pattern evolution in this group.

Finally, much remains to be investigated with respect to the molecular mechanisms by which *dsx* mediates polymorphic mimicry. In future work, I would study how *dsx* expression and binding activity regulate the development of distinct wing patterns and behaviors in *P. polytes*. This would also help us understand the contrasting patterns of *dsx* variation observed among

Papilio lineages, and whether these genetic signatures represent distinct functional mechanisms underlying polymorphic mimicry. My genomic analyses revealed signatures of high linkage disequilibrium around *dsx*, consistent with other recent works, but with linked-read sequence data, I could confirm whether chromosomal inversions are present around these regions.

Data Accessibility

Divergence and gene flow among Darwin's finches: A genome-wide view of adaptive radiation driven by interspecies allele sharing

- *Publication*: (Palmer and Kronforst, 2015)

Experimental field tests of Batesian mimicry in the swallowtail butterfly *Papilio polytes*

- *Publication*: (Palmer, Tan et al., *In press*)

The shared genetic basis of mimicry in swallowtail butterflies: common ancestry or independent evolution?

- *Publication*: (Palmer and Kronforst, *In review*)

References

Abbott R., Albach D., Ansell S., Arntzen J.W., Baird S.J.E., et al. 2013. Hybridization and speciation. J Evol Biol 26:229-46.

Abzhanov A., Protas M., Grant B.R., Grant P.R., et al. 2004. Bmp4 and morphological variation of beaks in Darwin's finches. Science 305:1462-5.

Abzhanov A., Kuo W.P., Hartmann C., Grant B.R., et al. 2006. The calmodulin pathway and evolution of elongated beak morphology in Darwin's finches. Nature 442:563-7.

Altschul S.F., Gish W., Miller W., Myers E.W., Lipman D.J., 1990. Basic local alignment search tool. Journal of Molecular Biology 215:403-410.

Barrett J.C., Fry B., Maller J., Daly M.J., 2004. Haploview: analysis and visualization of LD and haplotype maps. Bioinformatics 21:263-265.

Barrett R.D., Hoekstra H.E. 2011. Molecular spandrels: tests of adaptation at the genetic level. Nature Rev Genet 12:767-80.

Bates, H. W. 1862. Contributions to an insect fauna of the Amazon valley. Lepidoptera: Heliconidae. Trans. Linn. Soc. Lond. 23:495-566.

Benjamini Y., and Hochberg Y., 1995. Controlling the false discovery rate: a practical and powerful approach to multiple testing. Journal of the royal statistical society Series B (Methodological):289-300.

Bolger A.M., Lohse M., Usadel B., 2014. Trimmomatic: a flexible trimmer for Illumina sequence data. Bioinformatics 30:2114-2120.

Brawand D., Wagner C.E., Li Y.I., Malinsky M., et al. 2014. The genomic substrate for adaptive radiation in African cichlid fish. Nature 513:375-81.

Browning S.R., and Browning B.L., 2007. Rapid and accurate haplotype phasing and missing-data inference for whole-genome association studies by use of localized haplotype clustering. The American Journal of Human Genetics 81:1084-1097.

Burtis K.C., and Baker B.S., 1989. Drosophila *doublesex* gene controls somatic sexual differentiation by producing alternatively spliced mRNAs encoding related sex-specific polypeptides. Cell 56:997-1010.

Caley, M. J., and D. Schluter. 2003. Predators favour mimicry in a tropical reef fish. Proc. R. Soc. Lond.B. Biol. Sci. 270:667-672.

Castelletta, M., Thiollay, J.M. and Sodhi, N.S. 2005. The effects of extreme forest fragmentation on the bird community of Singapore Island. Biol. Cons. 121:135-155.

Chai, P. 1986. Field observations and feeding experiments on the responses of rufous-tailed jacamars (*Galbula ruficauda*) to free-flying butterflies in a tropical rainforest. Biol. J Linn. Soc. 29:161-189.

Charlesworth, D., and Charlesworth, B. 1975. Theoretical genetics of Batesian mimicry II. Evolution of supergenes. J. Theor. Biol. 55:305-324.

Clarke C., and Sheppard P., 1960. The genetics of *Papilio dardanus*, Brown. III. Race antinorii from Abyssinia and race meriones from Madagascar. Genetics 45:683.

Clarke C., and Sheppard P., 1962. The genetics of the mimetic butterfly *Papilio glaucus*. Ecology:159-161.

Clarke C.A., Sheppard P.M., Thornton I.W., 1968. The genetics of the mimetic butterfly *Papilio memnon* L. Philosophical Transactions of the Royal Society of London B: Biological Sciences 254:37-89.

Clarke C.A., and Sheppard P.M., 1972. The genetics of the mimetic butterfly *Papilio polytes* L. Philosophical Transactions of the Royal Society of London B: Biological Sciences 263:431-458.

Condamine F.L., Sperling F.A.H., Wahlberg N., Rasplus J.Y., Kergoat G.J., 2012. What causes latitudinal gradients in species diversity? Evolutionary processes and ecological constraints on swallowtail biodiversity. Ecology letters 15:267-277.

Cott, H.B. 1940. Adaptive coloration in animals. Methuen; London. pp. 292-294.

Danecek P., Auton A., Abecasis G., Albers C.A., Banks E., DePristo M.A., Handsaker R.E., Lunter G., Marth G.T., Sherry S.T., 2011. The variant call format and VCFtools. Bioinformatics 27:2156-2158.

Darwin C.R. 1845. Journal of Researches Into the Natural History and Geology of the Countries Visited During the Voyage of H.M.S. Beagle Round the World London: John Murray.

Darwin C.R. 1859. On the Origin of Species by Means of Natural Selection, or the Preservation of Favoured Races in the Struggle for Life London: John Murray.

Darwin C.R., and Wallace A.R. 1858. On the tendency of species to form varieties; and on the perpetuation of varieties and species by natural means of selection. Zool J Linn Soc 3: 46-50.

Dee C.T., Szymoniuk C.R., Mills P.E., Takahashi T. 2013. Defective neural crest migration revealed by a Zebrafish model of ALX1-related frontonasal dysplasia. Hum Mol Genet 22:239-51.

De León L.F., Raeymaekers J.A.M., Bermingham E., Podos J., Herrel A., et al. 2011. Exploring Possible Human Influences on the Evolution of Darwin's Finches. Evolution 65:2258-72.

Dell'Aglio, D. D., Stevens, M. and Jiggins, C. D. 2016. Avoidance of an aposematically coloured butterfly by wild birds in a tropical forest. Ecol. Entomol. 41:627-632.

Durand E.Y., Patterson N., Reich D., Slatkin M. 2011. Testing for ancient admixture between closely related populations. Mol Biol Evol 28:2239-52.

Ellegren H., Smeds L., Burri R., Olason P.I., Backstrom N., et al. 2012. The genomic landscape of species divergence in Ficedula flycatchers. Nature 491:756-60.

Ellegren, H., 2014. Genome sequencing and population genomics in non-model organisms. Trends in ecology and evolution 29:51-63.

Endler, J.A. 1991. Interactions between predators and prey. In: Behavioural Ecology, 3rd edn (J. R. Krebs and N. B. Davies, eds), pp. 169–196. Blackwell, Oxford, UK.

Endler, J. A. 1993. The color of light in forests and its implications. Ecol. Monogr. 63:1-27.

Ezawa K., Ikeo K., Gojobori T., Saitou N., 2010. Evolutionary pattern of gene homogenization between primate-specific paralogs after human and macaque speciation using the 4-2-4 method. Molecular biology and evolution 27:2152-2171.

Ezawa K., Ota S., Saitou N., 2006. Genome-wide search of gene conversions in duplicated genes of mouse and rat. Molecular biology and evolution 23:927-940.

Faria, R., and A. Navarro. 2010. Chromosomal speciation revisited: rearranging theory with pieces of evidence. Trends in Ecology and Evolution 25:660-669.

Farrington H.L., Lawson L.P., Clark C.M., Petren K. 2014. The evolutionary history of Darwin's finches: speciation, gene flow, and introgression in a fragmented landscape. Evolution 68:2932-44.

Finkbeiner, S. D., Briscoe, A. D. and Mullen, S. P. 2017a. Complex dynamics underlie the evolution of imperfect wing pattern convergence in butterflies. Evolution 71:949-959.

Finkbeiner, S. D., Briscoe, A. D. and Reed, R. D. 2012. The benefit of being a social butterfly: communal roosting deters predation. Proc. R. Soc. Lond.B. Biol. Sci. 279:2769-2776.

Finkbeiner, S. D., Briscoe, A. D. and Reed, R. D. 2014. Warning signals are seductive: relative contributions of color and pattern to predator avoidance and mate attraction in *Heliconius* butterflies. Evolution 68:3410-3420.

Finkbeiner, S. D., Fishman, D. A., Osorio, D. and Briscoe, A. D. 2017b. Ultraviolet and yellow reflectance but not fluorescence is important for visual discrimination of conspecifics by *Heliconius erato*. J Exp Biol 220:1267-1276.

Finkbeiner, S. D., Salazar, P., Nogales, S., Rush, C., Briscoe, A. D., Hill, R. I., Kronforst, M. R., Willmott, K. R., and Mullen, S. P. 2018. Frequency-dependence shapes the adaptive landscape of imperfect Batesian mimicry. Proc. R. Soc. Lond.B. Biol. Sci. 285:20172786.

Fontaine M.C., Pease J.B., Steele A., Waterhouse R.M., et al. 2015. Extensive introgression in a malaria vector species complex revealed by phylogenomics. Science 347:1258524.

Fouet C., Gray E., Besansky N.J., Costantini C. 2012. Adaptation to aridity in the malaria mosquito *Anopheles gambiae*: chromosomal inversion polymorphism and body size influence resistance to desiccation. PLoS One 7:e34841.

Fryer, J. 1913. Field-observations on the enemies of butterflies in Ceylon. In: Proc. Zool. Soc. Lond., Vol. 83. pp. 613-619.

Fryer, J. C. F. 1914. An investigation by pedigree breeding into the polymorphism of *Papilio polytes*, L. Phil. Trans. R. Soc. Lond. B 204:227-254.

Fukushima, K., Fang, X., Alvarez-Ponce, D., Cai, H., Carretero-Paulet, L., Chen, C., Chang, T.H., Farr, K.M., Fujita, T., Hiwatashi, Y. and Hoshi, Y., 2017. Genome of the pitcher plant *Cephalotus* reveals genetic changes associated with carnivory. Nature ecology and evolution 1:0059.

Gibbs H.L. and Grant P.R. 1987. Oscillating selection on Darwin's finches. Nature 327:511-3.

Gittleman, J. L., and Harvey, P. H. 1980. Why are distasteful prey not cryptic? Nature 286:149-150.

Gompel, N., Prud'homme, B., Wittkopp, P.J., Kassner, V.A. and Carroll, S.B. 2005. Chance caught on the wing: *cis*-regulatory evolution and the origin of pigment patterns in *Drosophila*. Nature 433:481–487.

Grant B.R., and Grant P.R. 1993. Evolution of Darwin's finches caused by a rare climatic event. Proc R Soc Lond B 251:111-7.

Grant P.R., and Grant B.R. 2002. Unpredictable evolution in a 30-year study of Darwin's finches. Science 296:707-11.

Grant P.R. 1993. Hybridization of Darwin's Finches on Isla Daphne Major, Galapagos. Phil Trans R Soc Lond B 340:127-39.

Grant P.R., and Grant B.R. 2010. Conspecific versus heterospecific gene exchange between populations of Darwin's finches. Phil Trans R Soc Lond B 365:1065-76.

Grant P.R., and Grant B.R. 1997a. Hybridization, sexual imprinting, and mate choice. Am Nat 149:1-28.

Grant P.R., and Grant B.R. 1997b. Mating patterns of Darwin's Finch hybrids determined by song and morphology. Biol J Linn Soc 60:317-43.

Grant B.R., and Grant P.R. 1998. Hybridization and speciation in Darwin's finches: the role of sexual imprinting on a culturally transmitted trait. In Howard DJ, Berlocher SH, eds; Endless forms: species and speciation. New York: Oxford Univ. Press. p 404–22.

Grant P.R., Grant B.R., Markert J.A., Keller L.F., et al. 2004. Convergent evolution of Darwin's finches caused by introgressive hybridization and selection. Evolution 58:1588-99.

Grant P.R., and Grant B.R. 2014. 40 Years of Evolution: Darwin's Finches on Daphne Major Island Princeton, NJ: Princeton University Press.

Gray E.M., Rocca K.A.C., Costantini C., Besansky N.J. 2009. Inversion 2La is associated with enhanced desiccation resistance in Anopheles gambiae. Malaria J 8:215.

Green R.E., Krause J., Briggs A.W., Maricic T., et al. 2010. A draft sequence of the Neandertal genome. Science 328:710-22.

Guilford, T. 1990. The evolution of aposematism. In: Insect Defenses: Adaptive Mechanisms and Strategies of Prey and Predators (D. L. Evans and J. O. Schmidt, eds), pp. 23–62. State University of New York Press, Albany.

Harrison, M.C., Jongepier, E., Robertson, H.M., Arning, N., Bitard-Feildel, T., Chao, H., Childers, C.P., Dinh, H., Doddapaneni, H., Dugan, S. and Gowin, J., 2018. Hemimetabolous genomes reveal molecular basis of termite eusociality. Nature ecology and evolution 2:557.

Hart N.S., Partridge J.C., Cuthill I.C. and Bennett A.T.D. 2000. Visual pigments, oil droplets, ocular media and cone photoreceptor distribution in two species of passerine bird: the blue tit (*Parus caeruleus* L.) and the blackbird (*Turdus merula* L.). J. Comp. Physiol. A 186:375-387.

Heliconius Genome Consortium. 2012. Butterfly genome reveals promiscuous exchange of mimicry adaptations among species. Nature 487:94-8.

Hendry A.P., Grant P.R., Grant B.R., Ford H.A., Brewer M.J., et al. 2006. Possible human impacts on adaptive radiation: beak size bimodality in Darwin's finches. Proc R Soc Lond B 273:1887-94.

Ho, S., Schachat, S. R., Piel, W. H. and Monteiro, A. 2016. Attack risk for butterflies changes with eyespot number and size. R. Soc. Open Sci. 3:150614.

Hoekstra H.E., and Coyne J.A. 2007. The locus of evolution: evo devo and the genetics of adaptation. Evolution 61:995-1016.

Hoffmann, A. A., and L. H. Rieseberg. 2008. Revisiting the impact of inversions in evolution: from population genetic markers to drivers of adaptive shifts and speciation?. Annual review of ecology, evolution, and systematics 39:21-42.

Huber S.K., De León L.F., Hendry A.P., Bermingham E., Podos J. 2007. Reproductive isolation of sympatric morphs in a population of Darwin's finches. Proc R Soc Lond B 274:1709-14.

Huerta-Sanchez E., Jin X., Asan, Bianba Z., et al. 2014. Altitude adaptation in Tibetans caused by introgression of Denisovan-like DNA. Nature 512:194-7.

Huheey, J.E. 1976. Studies in warning coloration and mimicry. VII. Evolutionary consequences of a Batesian-Müllerian spectrum: A model for Müllerian mimicry. Evolution. 30:86-93.

Ibáñez-Álamo, J., R. D. Magrath, J. Oteyza, A. Chalfoun, T. Haff, K. Schmidt, R. Thomson, and T. Martin. 2015. Nest predation research: recent findings and future perspectives. J. Ornithol. 156:247-262.

Jain, A., Lim, F.K. and Webb, E.L. 2017. Species-habitat relationships and ecological correlates of butterfly abundance in a transformed tropical landscape. Biotropica, 49:355-364.

Jarvis E.D., Mirarab S., Aberer A.J., Li B., et al. 2015. Phylogenomic analyses data of the avian phylogenomics project. Gigascience 4:4.

Johki, Y. 1983. Studies on avoidance of predation by colouration in insects. Doc. diss, Kyoto Univ., Kyoto.

Johki, Y., Kon, M. and Hidaka, T. 1986. Feeding experiments using the red avadavat, *Amandava amandava*, with reference to the effectiveness of Batesian mimicry. Mem. Fac. Sci. Kyoto Univ. (Ser. Biol.) 11:29-42.

Jones F.C., Grabherr M.G., Chan Y.F., Russell P., et al. 2012. The genomic basis of adaptive evolution in threespine sticklebacks. Nature 484:55-61.

Joron, M., Papa, R., Beltrán, M., Chamberlain, N., Mavárez, J., Baxter, S., Abanto, M., Bermingham, E., Humphray, S.J., Rogers, J. and Beasley, H., 2006. A conserved supergene locus controls colour pattern diversity in *Heliconius* butterflies. PLoS biology 4:e303.

Joron M., Frezal L., Jones R.T., Chamberlain N.L., et al. 2011. Chromosomal rearrangements maintain a polymorphic supergene controlling butterfly mimicry. Nature 477:203-6.

Joyce D.A., Lunt D.H., Genner M.J., Turner G.F., Bills R., et al. 2011. Repeated colonization and hybridization in Lake Malawi cichlids. Current Biology 21:R108-R9.

Kajitani R., Toshimoto K., Noguchi H., Toyoda A., Ogura Y., Okuno M., Yabana M., Harada M., Nagayasu E., Maruyama H., 2014. Efficient de novo assembly of highly heterozygous genomes from whole-genome shotgun short reads. Genome research 24:1384-1395.

Katoh K., Misawa K., Kuma Ki, Miyata T., 2002. MAFFT: a novel method for rapid multiple sequence alignment based on fast Fourier transform. Nucleic acids research 30:3059-3066.

Kearse M., Moir R., Wilson A., Stones-Havas S., Cheung M., Sturrock S., Buxton S., Cooper A., Markowitz S., Duran C., 2012. Geneious Basic: an integrated and extendable desktop software platform for the organization and analysis of sequence data. Bioinformatics 28:1647-1649.

Kent W.J., 2002. BLAT—the BLAST-like alignment tool. Genome research 12:656-664.

Kijimoto T., Moczek A.P., Andrews J., 2012. Diversification of *doublesex* function underlies morph-, sex-, and species-specific development of beetle horns. Proceedings of the National Academy of Sciences 109:20526-20531.

Kim, K. W., C. Bennison, N. Hemmings, L. Brookes, L. L. Hurley, S. C. Griffith, T. Burke, T. R. Birkhead, and J. Slate. 2017. A sex-linked supergene controls sperm morphology and swimming speed in a songbird. Nature ecology and evolution 1.

Kimura K-i, Hachiya T., Koganezawa M., Tazawa T., Yamamoto D., 2008. *Fruitless* and *doublesex* coordinate to generate male-specific neurons that can initiate courtship. Neuron 59:759-769.

Kirkpatrick M., and Barton N.. 2006. Chromosome inversions, local adaptation and speciation. Genetics 173:419-34.

Kirkpatrick, M. 2010. How and why chromosome inversions evolve. PLoS biology, 8:e1000501.

Kitamura T., and Imafuku M., 2010. Behavioral Batesian Mimicry Involving lntraspecific Polymorphism in the Butterfly *Papilio polytes*. Zoological science 27:217-221.

Kitamura T., and Imafuku M., 2015. Behavioural mimicry in flight path of Batesian intraspecific polymorphic butterfly *Papilio polytes*. Proceedings of the Royal Society B: Biological Sciences 282:20150483.

Koch P.B., and Behnecke B., 2000. The molecular basis of melanism and mimicry in a swallowtail butterfly. Current Biology 10:591-594.

Komata S., Lin C-P, Iijima T., Fujiwara H., Sota T., 2016. Identification of *doublesex* alleles associated with the female-limited Batesian mimicry polymorphism in *Papilio memnon*. Scientific reports 6.

Korunes K.L., and Noor M.A., 2017. Gene conversion and linkage: effects on genome evolution and speciation. Molecular ecology 26:351-364.

Krebs, R.A., and West, D.A. 1988. Female mate preference and the evolution of female-limited Batesian mimicry. Evolution 42:1101–1104.

Kronforst, M.R., Barsh, G.S., Kopp, A., Mallet, J., Monteiro, A., Mullen, S.P., Protas, M., Rosenblum, E.B., Schneider, C.J. and Hoekstra, H.E., 2012. Unraveling the thread of nature's tapestry: the genetics of diversity and convergence in animal pigmentation. Pigment cell and melanoma research 25:411-433.

Kuchta, S. R. 2005. Experimental support for aposematic coloration in the salamander *Ensatina eschscholtzii xanthoptica*: implications for mimicry of Pacific newts. Copeia 2005:265-271.

Kunte, K. 2009. The diversity and evolution of Batesian mimicry in *Papilio* swallowtail butterflies. Evolution 63:2707-2716.

Kunte, K., Zhang, W., Tenger-Trolander, A., Palmer, D. H., Martin, A., Reed, R. D., Mullen, S. P. and Kronforst, M. R. 2014. *doublesex* is a mimicry supergene. Nature 507:229-232.

Küpper, C., Stocks, M., Risse, J.E., dos Remedios, N., Farrell, L.L., McRae, S.B., Morgan, T.C., Karlionova, N., Pinchuk, P., Verkuil, Y.I. and Kitaysky, A.S., 2016. A supergene determines highly divergent male reproductive morphs in the ruff. Nature genetics 48:79.

Lack D. 1947. Darwin's Finches: Cambridge Univ. Press.

Lamichhaney S., Berglund J., Almen M.S., Maqbool K., et al. 2015. Evolution of Darwin's finches and their beaks revealed by genome sequencing. Nature 518:371-5.

Lamichhaney, S., G. Fan, F. Widemo, U. Gunnarsson, D. S. Thalmann, M. P. Hoeppner, S. Kerje et al. 2016. Structural genomic changes underlie alternative reproductive strategies in the ruff (*Philomachus pugnax*). Nature Genetics 48:84.

Langmead B., and Salzberg S.L., 2012. Fast gapped-read alignment with Bowtie 2. Nature methods 9:357-359.

Lee Y.W., Gould B.A., Stinchcombe J.R.. 2014. Identifying the genes underlying quantitative traits: a rationale for the QTN programme. Aob Plants 6.

Letunic I., and Bork P., 2006. Interactive Tree Of Life (iTOL): an online tool for phylogenetic tree display and annotation. Bioinformatics 23:127-128.

Li, J., Cocker, J.M., Wright, J., Webster, M.A., McMullan, M., Dyer, S., Swarbreck, D., Caccamo, M., van Oosterhout, C. and Gilmartin, P.M., 2016. Genetic architecture and evolution of the S locus supergene in *Primula vulgaris*. Nature plants 2:16188.

Lindström, L., Alatalo, R. V., Mappes, J. 1997. Imperfect Batesian mimicry—the effects of the frequency and the distastefulness of the model. Proc. R. Soc. B. Biol. Sci. 264:149-153.

Liu K.J., Steinberg E., Yozzo A., Song Y., et al. 2015. Interspecific introgressive origin of genomic diversity in the house mouse. Proc Natl Acad Sci USA 112:196-201.

Lövei, G. L. and Ferrante, M. 2017. A review of the sentinel prey method as a way of quantifying invertebrate predation under field conditions. Insect Sci. 24:528-542.

Low, X. H., and Monteiro, A. 2018. Dorsal forewing white spots of male *Papilio polytes* (Lepidoptera: Papilionidae) not maintained by female mate choice. J. of Insect Behav. 1-13.

Lowry, D. B., and J. H. Willis. 2010. A widespread chromosomal inversion polymorphism contributes to a major life-history transition, local adaptation, and reproductive isolation. PLoS Biology 8:1-14.

Mallarino R., Grant P.R., Grant B.R., Herrel A., et al. 2011. Two developmental modules establish 3D beak-shape variation in Darwin's finches. Proc Natl Acad Sci USA 108: 4057-62.

Marchand, M. N., J. A. Litvaitis, T. J. Maier, and R. M. DeGraaf. 2002. Use of artificial nests to investigate predation on freshwater turtle nests. Wildl. Soc. Bull. 1092-1098.

Marshall, G. A. 1909. V. Birds as a factor in the production of mimetic resemblances among butterflies. Ecol. Entomol. 57:329-384.

Martin S.H., Dasmahapatra K.K., Nadeau N.J., Salazar C., et al. 2013. Genome-wide evidence for speciation with gene flow in *Heliconius* butterflies. Genome Res 23:1817-28.

Martin A., and Orgogozo V., 2013. The loci of repeated evolution: a catalog of genetic hotspots of phenotypic variation. Evolution 67:1235-1250.

Martin, C.H., Cutler, J.S., Friel, J.P., Dening Touokong, C., Coop, G. and Wainwright, P.C., 2015. Complex histories of repeated gene flow in Cameroon crater lake cichlids cast doubt on one of the clearest examples of sympatric speciation. Evolution 69:1406-1422.

McGhee G.R., 2011. Convergent evolution: limited forms most beautiful: MIT Press.

McKenna A., Hanna M., Banks E., Sivachenko A., Cibulskis K., Kernytsky A., Garimella K., Altshuler D., Gabriel S., Daly M., 2010. The Genome Analysis Toolkit: a MapReduce framework for analyzing next-generation DNA sequencing data. Genome research 20:1297-1303.

Merrill, R. M., Wallbank, R. W., Bull, V., Salazar, P. C., Mallet, J., Stevens, M. and Jiggins, C. D. 2012. Disruptive ecological selection on a mating cue. Proc. R. Soc. B. Biol. Sci. 279:4907-4913.

Nadeau, N. J., and Jiggins, C. D. 2010. A golden age for evolutionary genetics? Genomic studies of adaptation in natural populations. Trends Genet 26:484-92.

Nishikawa, H., Iga, M., Yamaguchi, J., Saito, K., Kataoka, H., Suzuki, Y., Sugano, S. and Fujiwara, H. 2013. Molecular basis of wing coloration in a Batesian mimic butterfly, *Papilio polytes*. Sci. Rep. 3.

Nishikawa, H., Iijima, T., Kajitani, R., Yamaguchi, J., Ando, T., Suzuki, Y., Sugano, S., Fujiyama, A., Kosugi, S. and Hirakawa, H. 2015. A genetic mechanism for female-limited Batesian mimicry in *Papilio* butterfly. Nat. Genet. 47:405-409.

Norris L.C., Main B.J., Lee Y., Collier T.C., et al. 2015. Adaptive introgression in an African malaria mosquito coincident with the increased usage of insecticide-treated bed nets. Proc Natl Acad Sci USA 112:815-20.

Ohsaki, N. 1995. Preferential predation of female butterflies and the evolution of Batesian mimicry. Nature 378:173.

Olsson P., Lind O., Kelber A. 2015. Bird colour vision: behavioral thresholds reveal receptor noise. J. Exp. Biol. 218:184-193.

Palmer, D.H. and Kronforst, M.R., 2015. Divergence and gene flow among Darwin's finches: A genome-wide view of adaptive radiation driven by interspecies allele sharing. Bioessays 37:968-974.

Papa, R., Martin, A. and Reed, R.D., 2008. Genomic hotspots of adaptation in butterfly wing pattern evolution. Current opinion in genetics and development 18:559-564.

Pardo-Diaz C., Salazar C., Baxter S.W., Merot C., et al. 2012. Adaptive introgression across species boundaries in *Heliconius* butterflies. Plos Genet 8:e1002752.

Petren K., Grant P.R., Grant B.R., Keller L.F. 2005. Comparative landscape genetics and the adaptive radiation of Darwin's finches: the role of peripheral isolation. Mol Ecol 14:2943-57.

Pfennig, D. W., W. R. Harcombe, and K. S. Pfennig. 2001. Frequency-dependent Batesian mimicry. Nature 410:323.

Podos J. 2001. Correlated evolution of morphology and vocal signal structure in Darwin's finches. Nature 409:185-8.

Poelstra J.W., Vijay N., Bossu C.M., Lantz H., Ryll B., et al. 2014. The genomic landscape underlying phenotypic integrity in the face of gene flow in crows. Science 344:1410-4.

Prud'homme, B., Gompel, N., Rokas, A., Kassner, V.A., Williams, T.M., Yeh, S.-D., True, J.R. and Carroll, S.B. 2006. Repeated morphological evolution through *cis*-regulatory changes in a pleiotropic gene. Nature 440:1050–1053.

Prüfer K., Racimo F., Patterson N., Jay F., Sankararaman S., et al. 2014. The complete genome sequence of a Neanderthal from the Altai Mountains. Nature 505:43-9.

Purcell S., Neale B., Todd-Brown K., Thomas L., Ferreira M.A., Bender D., Maller J., Sklar P., De Bakker P.I., Daly M.J., 2007. PLINK: a tool set for whole-genome association and population-based linkage analyses. The American Journal of Human Genetics 81:559-575.

Qvarnström A., and Bailey R.I. 2009. Speciation through evolution of sex-linked genes. Heredity 102:4-15.

R Core Team 2014. R: A language and environment for statistical computing. R Foundation for Statistical Computing, Vienna, Austria. ISBN 3-900051-07-0, URL http://www.R-project.org/.

Rabosky A.R.D., Cox C.L., Rabosky D.L., Title P.O., Holmes I.A., Feldman A., McGuire J.A., 2016. Coral snakes predict the evolution of mimicry across New World snakes. Nature communications 7.

Rands C., Darling A., Fujita M., Kong L., et al. 2013. Insights into the evolution of Darwin's finches from comparative analysis of the *Geospiza magnirostris* genome sequence. BMC Genomics 14:95.

Rausher, M.D. and Delph, L.F., 2015. Commentary: When does understanding phenotypic evolution require identification of the underlying genes? Evolution 69:1655-1664.

Reed, R.D., Papa, R., Martin, A., Hines, H.M., Counterman, B.A., Pardo-Diaz, C.et al. 2011. *Optix* drives the repeated convergent evolution of butterfly wing pattern mimicry. Science 333:1137–1141.

Rieseberg L.H., Raymond O., Rosenthal D.M., Lai Z., Livingstone K., et al. 2003. Major ecological transitions in wild sunflowers facilitated by hybridization. Science 301:1211-6.

Ritland, D. B. and Brower, L. P. 1991. The viceroy butterfly is not a Batesian mimic. Nature 350:497-498.

Rockman M.V. 2012. The QTN program and the alleles that matter for evolution: all that's gold does not glitter. Evolution 66:1-17.

Roper, T. and Redston, S. 1987. Conspicuousness of distasteful prey affects the strength and durability of one-trial avoidance learning. Anim. Behav. 35:739-747.

Rosenblum, E.B., Parent, C.E. and Brandt, E.E., 2014. The molecular basis of phenotypic convergence. Annual Review of Ecology, Evolution, and Systematics 45:203-226.

Ruxton, G. D., Sherratt, T. N., and Speed, M. P. 2004. Avoiding attack: the evolutionary ecology of crypsis, warning signals and mimicry. Oxford University Press. pp.139-163.

San-Jose, L.M. and Roulin, A., 2017. Genomics of coloration in natural animal populations. Phil. Trans. R. Soc. B 372:20160337.

Saporito, R. A., R. Zuercher, M. Roberts, K. G. Gerow, and M. A. Donnelly. 2007. Experimental evidence for aposematism in the dendrobatid poison frog *Oophaga pumilio*. Copeia 2007:1006-1011.

Savage W.K. and Mullen S.P., 2009. A single origin of Batesian mimicry among hybridizing populations of admiral butterflies (*Limenitis arthemis*) rejects an evolutionary reversion to the ancestral phenotype. Proceedings of the Royal Society of London B: Biological Sciences 276:2557-2565.

Sawyer S., 1999. GENECONV: A computer package for the statistical detection of gene conversion. http://www/ math wustl edu/~ sawyer.

Schuler, W. and Hesse, E. 1985. On the function of warning coloration: a black and yellow pattern inhibits prey-attack by naive domestic chicks. Behav. Ecol. and Sociobiol. 16:249-255.

Schwander, T., Libbrecht, R. and Keller, L., 2014. Supergenes and complex phenotypes. Current Biology 24:R288-R294.

Scriber J.M., Hagen R.H., Lederhouse R.C., 1996. Genetics of mimicry in the tiger swallowtail butterflies, *Papilio glaucus* and *P. canadensis* (Lepidoptera: Papilionidae). Evolution 50:222-236.

Seymoure, B.M. and Aiello, A. 2015. Keeping the band together: evidence for false boundary disruptive coloration in a butterfly. J. Evol. Biol. 28:1618-1624.

Shapiro, M.D., Marks, M.E., Peichel, C.L., Blackman, B.K., Nereng, K.S., Jónsson, B., Schluter, D. and Kingsley, D.M. 2004. Genetic and developmental basis of evolutionary pelvic reduction in threespine sticklebacks. Nature 428:717–723.

Smetacek, P. 2006. Some distasteful Asian Papilioninae (Papilionidae). J. Lepid. Soc. 60:82.

Smith, S. M. 1975. Innate recognition of coral snake pattern by a possible avian predator. Science 187:759-760.

Smith, S. M. 1977. Coral-snake pattern recognition and stimulus generalisation by naive great kiskadees (Aves: Tyrannidae). Nature 265:535.

Smith J., and Kronforst M.R. 2013. Do *Heliconius* butterfly species exchange mimicry alleles? Biol Lett 9:0130503.

Song Y., Endepols S., Klemann N., Richter D., et al. 2011. Adaptive introgression of anticoagulant rodent poison resistance by hybridization between old world mice. Curr Biol 21:1296-301.

Speed, M. P. 2000. Warning signals, receiver psychology and predator memory. Anim. Behav. 60:269-278.

Stamatakis A., 2014. RAxML version 8: a tool for phylogenetic analysis and post-analysis of large phylogenies. Bioinformatics 30:1312-1313.

Stapley J., Reger J., Feulner P.G.D., Smadja C., et al. 2010. Adaptation genomics: the next generation. Trends Ecol Evol 25:705-12.

Stern D.L. and Orgogozo V. 2008. The loci of evolution: how predictable is genetic evolution? Evolution 62:2155-77.

Stern D.L. and Orgogozo V. 2009. Is genetic evolution predictable? Science 323:746-51.

Stern D.L., 2013. The genetic causes of convergent evolution. Nature Reviews Genetics 14:751.

Stevens, M., Hardman, C.J. and Stubbins, C.L. 2008. Conspicuousness, not eye mimicry, makes "eyespots" effective antipredator signals. Behav. Ecol. 19:525-531.

Stuart-Fox, D. M., A. Moussalli, N. J. Marshall, and I. P. Owens. 2003. Conspicuous males suffer higher predation risk: visual modelling and experimental evidence from lizards. Animal Behav. 66:541-550.

Sturtevant, A. H. 1921. A case of rearrangement of genes in *Drosophila*. Proceedings of the National Academy of Sciences 7:235-237.

Su, S., Lim, M. and Kunte, K. 2015. Prey from the eyes of predators: Color discriminability of aposematic and mimetic butterflies from an avian visual perspective. Evolution 69:2985-2994.

Sulloway F. 1982. Darwin and his finches: The evolution of a legend. J Hist Biol 15:1-53.

Tanaka K., Barmina O., Sanders L.E., Arbeitman M.N., Kopp A., 2011. Evolution of sex-specific traits through changes in HOX-dependent *doublesex* expression. PLoS-Biology 9:1758.

Timmermans, M.J., Baxter, S.W., Clark, R., Heckel, D.G., Vogel, H., Collins, S., Papanicolaou, A., Fukova, I., Joron, M., Thompson, M.J. and Jiggins, C.D., 2014. Comparative genomics of the mimicry switch in *Papilio dardanus*. Proc. R. Soc. B 281:20140465.

Timmermans, M.J., Thompson, M.J., Collins, S. and Vogler, A.P., 2017. Independent evolution of sexual dimorphism and female-limited mimicry in swallowtail butterflies (*Papilio dardanus* and *Papilio phorcas*). Molecular ecology 26:1273-1284.

Turner, J. R. 1978. Why male butterflies are non-mimetic: natural selection, sexual selection, group selection, modification and sieving. Biol. J. Linn. Soc. 10:385-432.

Turner S.D., 2014. qqman: an R package for visualizing GWAS results using QQ and manhattan plots. BioRxiv:005165.

Tuttle, E. M., A. O. Bergland, M. L. Korody, M. S. Brewer, D. J. Newhouse, P. Minx, M. Stager et al. 2016. Divergence and functional degradation of a sex chromosome-like supergene. Current Biology 26:344-350.

Uésugi, K. 1996. The adaptive significance of Batesian mimicry in the swallowtail butterfly, *Papilio polytes* (Insecta, Papilionidae): associative learning in a predator. Ethology 102:762-775.

Uz E., Alanay Y., Aktas D., Vargel I., et al. 2010. Disruption of *ALX1* causes extreme microphthalmia and severe facial clefting: expanding the spectrum of autosomal-recessive *ALX*-related frontonasal dysplasia. Am J Hum Genet 86:789-96.

Vernot B., and Akey J.M. 2014. Resurrecting Surviving Neandertal Lineages from Modern Human Genomes. Science 343:1017-21.

Vignieri, S. N., J. G. Larson, and H. E. Hoekstra. 2010. The selective advantage of crypsis in mice. Evolution 64:2153-2158.

Vorobyev, M. and Osorio, D. 1998. Receptor noise as a determinant of colour thresholds. Proc. R. Soc. Lond. B 265:351–358.

Wallace, A. R. 1865. On the phenomena of variation and geographical distribution as illustrated by the Papilionidae of the Malayan region. Trans. Linn. Soc. Lond. 25:1-71.

Wang, J., Wurm, Y., Nipitwattanaphon, M., Riba-Grognuz, O., Huang, Y.C., Shoemaker, D. and Keller, L., 2013. A Y-like social chromosome causes alternative colony organization in fire ants. Nature 493:664.

Wee, J. L. Q. and Monteiro, A. 2017. Yellow and the novel aposematic signal, red, protect *Delias* butterflies from predators. PloS ONE 12:e0168243.

Weir B.S., and Cockerham C.C., 1984. Estimating F-statistics for the analysis of population structure. evolution 38:1358-1370.

Wickham H, 2016. ggplot2: elegant graphics for data analysis: Springer.

Wickler, W. 1968. Mimicry in plants and animals. London, Weidenfeld and Nicolson. pp.60-110.

Williams T.M. and Carroll S.B., 2009. Genetic and molecular insights into the development and evolution of sexual dimorphism. Nature Reviews Genetics 10:797-804.

Zakharov E.V., Caterino M.S., Sperling F.A., 2004. Molecular phylogeny, historical biogeography, and divergence time estimates for swallowtail butterflies of the genus *Papilio* (Lepidoptera: Papilionidae). Systematic biology 53:193-215.

Zhan S., Zhang W., Niitepold K., Hsu J., et al. 2014. The genetics of monarch butterfly migration and warning colouration. Nature 514:317-21.

Zhang G., Parker P., Li B., Li H., et al. 2012. The genome of Darwin's Finch (*Geospiza fortis*). GigaScience: http://dx.doi.org/10.5524/100040.

Zhang G., Li B., Li C., Gilbert M.T., et al. 2014a. Comparative genomic data of the Avian Phylogenomics Project. Gigascience 3:26.

Zhang G., Li C., Li Q., Li B., et al. 2014b. Comparative genomics reveals insights into avian genome evolution and adaptation. Science 346:1311-20.

Zhang W., Westerman E., Nitzany E., Palmer S., Kronforst M.R., 2017. Tracing the origin and evolution of supergene mimicry in butterflies. Nature communications 8:1269.

Zhou X., Stephens M., 2012. Genome-wide efficient mixed-model analysis for association studies. Nature genetics 44:821-824.

Appendix

Table S1 | Sample information and sequencing statistics

Sample	Species	Morph	Origin	Raw reads (Gb)	Mean Depth
Pae 7	*P. aegeus*	Dark	Queensland, Australia	171.20	70.17
Pae8	*P. aegeus*	Dark	Queensland, Australia	70.69	28.97
Pae9	*P. aegeus*	Dark	Queensland, Australia	93.08	38.15
Pae12	*P. aegeus*	Dark	Queensland, Australia	101.22	41.49
Pae20	*P. aegeus*	Dark	Queensland, Australia	118.37	48.51
Pae21	*P. aegeus*	Dark	Queensland, Australia	116.94	47.92
Pae22	*P. aegeus*	Dark	Queensland, Australia	111.06	45.52
Pae23	*P. aegeus*	Dark	Queensland, Australia	114.40	46.88
Pae14	*P. aegeus*	Light	Iron Range, Queensland, Australia	157.90	64.71
Pae15	*P. aegeus*	Light	Iron Range, Queensland, Australia	136.44	55.92
Pae16	*P. aegeus*	Light	Iron Range, Queensland, Australia	145.69	59.71
Pae17	*P. aegeus*	Light	Iron Range, Queensland, Australia	109.06	44.70
Palc	*P. alcmenor*	-	Yunnan, China	90.00	36.89
Pas4	*P. ascalaphus*	-	Sulawesi, Indonesia	83.93	34.40
Pas5	*P. ascalaphus*	-	Sulawesi, Indonesia	119.95	49.16
Pas1	*P. ascalaphus*	-	Sulawesi, Indonesia	161.59	66.23
Pas3	*P. ascalaphus*	-	Sulawesi, Indonesia	129.49	53.07
Pas6	*P. ascalaphus*	-	Sulawesi, Indonesia	140.93	57.76
Pboo	*P. bootes*	-	Sichuan, China	125.08	51.26
Pcas1	*P. castor*	-	Yunnan, China	118.45	48.55
Pcas2	*P. castor*	-	Yunnan, China	125.10	51.27
Pgam1	*P. gambrisius*	-	Seram, Indonesia	126.08	51.67
Pgam2	*P. gambrisius*	-	Seram, Indonesia	75.95	31.13
Pgam3	*P. gambrisius*	-	Seram, Indonesia	146.02	59.84
Pis1	*P. iswara*	-	Lingga, Indonesia	124.84	51.16
Pmac1	*P. macilentus*	-	South Korea	127.97	52.45
N1	*P. memnon*	Band	Phrae, Thailand	103.56	42.44
N10	*P. memnon*	Band	Phrae, Thailand	208.83	85.58
N2	*P. memnon*	Band	Phrae, Thailand	105.04	43.05
N233	*P. memnon*	Band	Thailand	103.26	42.32
N234	*P. memnon*	Band	Thailand	100.69	41.27
N3	*P. memnon*	Band	Phrae, Thailand	116.42	47.72
N4	*P. memnon*	Band	Phrae, Thailand	96.57	39.58

N5	*P. memnon*	Band	Phrae, Thailand	113.97	46.71
N500	*P. memnon*	Band	Thailand	101.56	41.62
N502	*P. memnon*	Band	Thailand	105.59	43.27
N503	*P. memnon*	Band	Thailand	100.00	40.98
N505	*P. memnon*	Band	Thailand	100.74	41.29
N506	*P. memnon*	Band	Thailand	99.16	40.64
N507	*P. memnon*	Band	Thailand	101.25	41.50
N508	*P. memnon*	Band	Thailand	101.60	41.64
N510	*P. memnon*	Band	Thailand	99.57	40.81
N511	*P. memnon*	Band	Thailand	99.67	40.85
N512	*P. memnon*	Band	Thailand	104.61	42.87
N6	*P. memnon*	Band	Phrae, Thailand	114.66	46.99
N8	*P. memnon*	Band	Phrae, Thailand	231.99	95.08
N9	*P. memnon*	Band	Phrae, Thailand	291.28	119.38
N205	*P. memnon*	Patch	Thailand	103.03	42.23
N207	*P. memnon*	Patch	Thailand	107.40	44.01
N209	*P. memnon*	Patch	Thailand	175.90	72.09
N210	*P. memnon*	Patch	Thailand	112.61	46.15
N211	*P. memnon*	Patch	Thailand	98.32	40.29
N215	*P. memnon*	Patch	Thailand	100.82	41.32
N221	*P. memnon*	Patch	Thailand	103.80	42.54
N222	*P. memnon*	Patch	Thailand	102.37	41.96
N224	*P. memnon*	Patch	Thailand	122.02	50.01
Poe	*P. oenomaus*	-	Seram, Indonesia	120.32	49.31
Poe1	*P. oenomaus*	-	Seram, Indonesia	134.77	55.23
Poe2	*P. oenomaus*	-	Seram, Indonesia	136.43	55.91
Ppm1	*P. polymnestor*	-	Gurutalawa, Sri Lanka	113.42	46.48
Ppm2	*P. polymnestor*	-	Gurutalawa, Sri Lanka	139.87	57.32
Ppm3	*P. polymnestor*	-	Gurutalawa, Sri Lanka	126.03	51.65
Polytes1 (SRR1118145)	*P. polytes*	Mimetic	-	28.55	11.70
Polytes2 (SRR1118150)	*P. polytes*	Mimetic	-	28.68	11.76
Polytes3 (SRR1118152)	*P. polytes*	Mimetic	-	27.99	11.47
Cyrus1 (SRR1111718)	*P. polytes*	Non-mimetic	-	29.63	12.14
Cyrus2 (SRR1112070)	*P. polytes*	Non-mimetic	-	30.47	12.49
Cyrus3 (SRR1112619)	*P. polytes*	Non-mimetic	-	33.00	13.52
Ppro1	*P. protenor*	-	Guangxi, China	123.41	50.58
Ppro2	*P. protenor*	-	Guangxi, China	115.65	47.40

Ppro3	*P. protenor*	-	Guangxi, China	116.63	47.80
Ppro4	*P. protenor*	-	Guangxi, China	116.66	47.81
Ppro5	*P. protenor*	-	Guangxi, China	118.66	48.63
Ppro6	*P. protenor*	-	Yunnan, China	119.61	49.02
Ppro7	*P. protenor*	-	Yunnan, China	126.18	51.72
MKDP100	*P. rumanovia*	Blended	Philippines	28.18	11.55
MKDP101	*P. rumanovia*	Blended	Philippines	32.66	13.38
MKDP102	*P. rumanovia*	Blended	Philippines	26.54	10.88
MKDP20	*P. rumanovia*	Blended	Philippines	127.53	52.26
MKDP21	*P. rumanovia*	Blended	Philippines	127.16	52.11
MKDP22	*P. rumanovia*	Blended	Philippines	116.62	47.80
MKDP23	*P. rumanovia*	Blended	Philippines	125.09	51.26
MKDP24	*P. rumanovia*	Blended	Philippines	122.28	50.11
MKDP25	*P. rumanovia*	Blended	Philippines	128.83	52.80
MKDP27	*P. rumanovia*	Blended	Philippines	111.98	45.89
MKDP63	*P. rumanovia*	Blended	Philippines	35.43	14.52
MKDP82	*P. rumanovia*	Blended	Philippines	31.45	12.89
MKDP93	*P. rumanovia*	Blended	Philippines	36.50	14.96
MKDP98	*P. rumanovia*	Blended	Philippines	39.11	16.03
MKDP99	*P. rumanovia*	Blended	Philippines	37.73	15.46
MKDP11	*P. rumanovia*	Simple	Philippines	24.26	9.94
MKDP28	*P. rumanovia*	Simple	Philippines	117.21	48.04
MKDP29	*P. rumanovia*	Simple	Philippines	142.31	58.33
MKDP30	*P. rumanovia*	Simple	Philippines	136.90	56.11
MKDP31	*P. rumanovia*	Simple	Philippines	136.56	55.97
MKDP32	*P. rumanovia*	Simple	Philippines	141.00	57.79
MKDP33	*P. rumanovia*	Simple	Philippines	145.00	59.43
MKDP34	*P. rumanovia*	Simple	Philippines	128.34	52.60
MKDP35	*P. rumanovia*	Simple	Philippines	130.50	53.48
MKDP61	*P. rumanovia*	Simple	Philippines	23.22	9.52
MKDP85	*P. rumanovia*	Simple	Philippines	20.80	8.52
MKDP89	*P. rumanovia*	Simple	Philippines	26.93	11.04
MKDP94	*P. rumanovia*	Simple	Philippines	28.98	11.88
MKDP95	*P. rumanovia*	Simple	Philippines	32.48	13.31
MKDP96	*P. rumanovia*	Simple	Philippines	33.84	13.87
MKDP97	*P. rumanovia*	Simple	Philippines	30.14	12.35
MKDP10	*P. rumanovia*	White	Philippines	26.01	10.66
MKDP12	*P. rumanovia*	White	Philippines	27.02	11.07
MKDP18	*P. rumanovia*	White	Philippines	34.07	13.96
MKDP36	*P. rumanovia*	White	Philippines	137.28	56.26

MKDP37	*P. rumanovia*	White	Philippines	127.54	52.27
MKDP38	*P. rumanovia*	White	Philippines	133.27	54.62
MKDP39	*P. rumanovia*	White	Philippines	128.84	52.80
MKDP40	*P. rumanovia*	White	Philippines	125.44	51.41
MKDP41	*P. rumanovia*	White	Philippines	130.05	53.30
MKDP42	*P. rumanovia*	White	Philippines	199.75	81.86
MKDP43	*P. rumanovia*	White	Philippines	174.53	71.53
MKDP53	*P. rumanovia*	White	Philippines	29.03	11.90
MKDP58	*P. rumanovia*	White	Philippines	32.24	13.21
MKDP60	*P. rumanovia*	White	Philippines	26.78	10.97
MKDP62	*P. rumanovia*	White	Philippines	22.31	9.14
MKDP83	*P. rumanovia*	White	Philippines	25.91	10.62
Psat1	*P. sataspes*	-	Sulawesi, Indonesia	125.96	51.62
Psat2	*P. sataspes*	-	Sulawesi, Indonesia	156.40	64.10
Psat3	*P. sataspes*	-	Sulawesi, Indonesia	137.80	56.47
Ptai1	*P. taiwanus*	-	Nantou, Taiwan	141.53	58.00
Pty1	*P. tydeus*	-	Morotai, Indonesia	109.14	44.73
Pty2	*P. tydeus*	-	Morotai, Indonesia	117.87	48.31
Pty3	*P. tydeus*	-	Morotai, Indonesia	105.58	43.27
Pty4	*P. tydeus*	-	Morotai, Indonesia	105.83	43.37
Pty5	*P. tydeus*	-	Morotai, Indonesia	110.86	45.44
Pty6	*P. tydeus*	-	Morotai, Indonesia	108.07	44.29
Pwoo1	*P. woodfordi*	-	Bougainville, Papua New Guinea	83.19	34.10
Pwoo2	*P. woodfordi*	-	Bougainville, Papua New Guinea	104.99	43.03
Pwoo3	*P. woodfordi*	-	Bougainville, Papua New Guinea	105.40	43.20